Research Square

Preprints are preliminary reports that have not undergone peer review.
They should not be considered conclusive, used to inform clinical practice,
or referenced by the media as validated information.

Universal seropositivity, markers of recurrent reactivation, and a convergent T-cell response implicate cytomegalovirus in Susac syndrome

Nicholas Schwab

nicholas.schwab@ukmuenster.de

University of Münster https://orcid.org/0000-0001-5494-9885

Eva Dawin

Tilman Schneider-Hohendorf

University of Muenster https://orcid.org/0000-0002-3717-5176

Andreas Schulte-Mecklenbeck

Department of Neurology, University Hospital Freiburg

Markus Kraemer

Department of Neurology, Alfried Krupp Krankenhaus

Damon May

Adaptive Biotechnologies - 1165 Eastlake Ave E, Seattle, WA 98109 https://orcid.org/0000-0001-6902-3153

Christian Wünsch

University of Münster

Simon Falk

University of Münster

Jingyun Li

Body and Brain Institute Münster, Department of Neurology, University Hospital Münste

Lukas Kaufmann

Institute of Virology, University Hospital Münster

Antonios Katsounas

Department of Medicine, Knappschaft Kliniken University Hospital Bochum, Ruhr University Bochum

Eva Schumann

Body and Brain Institute Münster, Department of Neurology, University Hospital Münster

Steven Woodhouse

Adaptive Biotechnologies

Bryan Howie

Adaptive Biotechnologies

Mark Klinger

Adaptive Biotechnologies

Edward Osborne
Adaptive Biotechnologies

Jennifer Moy
Adaptive Biotechnologies

Bernhard Schlüter
UKM-Laboratory, University Hospital Münster

Todd Hardy
Department of Neurology, Concord Hospital, University of Sydney

Dimitri Hemelsoet
Ghent University Hospital https://orcid.org/0000-0001-5403-3092

Mariano Marrodan
Neurology Department, Fleni

Sven Jarius
Division of Neuroimmunology, Department of Neurology, University of Heidelberg

Klemens Ruprecht
Division of Neuroimmunology, Department of Neurology, University of Heidelberg

Brigitte Wildemann
University of Heidelberg

Beatrijs Wokke
Erasmus MC, University Medical Center Rotterdam

Adi Wilf-Yarkoni
Department of Neurology, Rabin Medical Center

Barbara Willekens
Translational Neurosciences, Laboratory for Experimental Hematology, University of Antwerp and Department of Neurology, Antwerp University Hospital https://orcid.org/0000-0002-5212-8837

Corinna Seliger
Ruhr University Bochum

Jan Bauer
Center for Brain Research, Medical University of Vienna https://orcid.org/0000-0001-5802-8047

Roland Liblau
Institut National de la Sante et de la Recherche Medicale https://orcid.org/0000-0001-5477-5475

Manfred Fobker
Center for Laboratory Medicine, University Hospital Muenster

Friedemann Paul
Charité University Medicine Berlin

Gerd Meyer zu Horste
University Hospital Münster https://orcid.org/0000-0002-4341-4719

Carolin Otto

Charité - Universitätsmedizin Berlin

Jan Dörr

Clinical and Experimental Research Center for Multiple Sclerosis, Department of Neurology, Charité - Universitätsmedizin Berlin

Marius Ringelstein

Center for Neurology, Department of Neuroimmunology and Neuromuscular Diseases, University Hospital and University Bonn

Joachim Kühn

University Hospital Münster

Harlan Robins

Adaptive Biotechnologies

Guy Laureys

University Hospital Ghent

Luisa Klotz

University Hospital Münster https://orcid.org/0000-0001-5439-9633

Sven Meuth

Body and Brain Institute Münster, Department of Neurology, University Hospital Münster

Heinz Wiendl

University Hospital of Münster https://orcid.org/0000-0003-4310-3432

Ilka Kleffner

Department of Neurology, Knappschaft Kliniken University Hospital Bochum, Ruhr University Bochum

Catharina Gross

Department of Neurology with Institute of Translational Neurology, University of Muenster https://orcid.org/0000-0002-4872-9189

Article

Keywords:

Posted Date: September 14th, 2026

DOI: https://doi.org/10.21203/rs.3.rs-11006811/v1

License: This work is licensed under a Creative Commons Attribution 4.0 International License. Read Full License

Additional Declarations: Yes there is potential Competing Interest. Competing interests N.S. declares no competing interests. E.D. declares no competing interests. T.S.-H. declares no competing interests. A.S.-M. declares no competing interests. M. Kraemer declares no competing interests. D.M. is an employee of Adaptive Biotechnologies and receives salary, stock, and options as part of their employment compensation outside of the submitted work. C.W. declares no competing interests. S.F. declares no

competing interests. J.L. declares no competing interests. L. Kaufmann declares no competing interests. A.K. declares no competing interests. E.M.S. declares no competing interests. S.W. is an employee of Adaptive Biotechnologies and receives salary, stock, and options as part of their employment compensation outside of the submitted work. B.H. is an employee of Adaptive Biotechnologies and receives salary, stock, and options as part of their employment compensation outside of the submitted work. M. Klinger is an employee of Adaptive Biotechnologies and receives salary, stock, and options as part of their employment compensation outside of the submitted work. E.J.O. is an employee of Adaptive Biotechnologies and receives salary, stock, and options as part of their employment compensation outside of the submitted work. J.M. is an employee of Adaptive Biotechnologies and receives salary, stock, and options as part of their employment compensation outside of the submitted work. B.S. declares no competing interests. T.A.H. received speaker honoraria, conference support, or scientific advisory board fees from Bayer-Schering, Bristol-Myers Squibb, Biogen-Idec, Merck, Novartis, Roche, UCB, Sanofi-Genzyme, Alexion, Sandoz, Teva, and Neuraxpharm. D.H. declares no competing interests. M.M. declares no competing interests. S.J. declares no competing interests. K.R. received research support from the European Union (821283-2), Stiftung Charité, the Guthy-Jackson Charitable Foundation, and the Arthur Arnstein Foundation, and speaker honoraria from Virion Serion and Novartis. B. Wildemann received research support from the Federal Ministry of Research, Technology and Space, the German Research Foundation (DFG), the Baden-Württemberg Ministry of Science, Research and Arts, Argenx, Novartis, and Roche, and honoraria and/or travel support from Alexion, Argenx, INSTAND, Neuraxpharm, Novartis, and Roche. B. Wokke received research support from Hansa Biopharma, none related to this study. A.W.-Y. declares no competing interests. B. Willekens received travel support to attend conferences and meetings from Biogen, Sanofi-Genzyme, Merck, Neuraxpharm, Novartis, Roche, UCB, EAN, European Charcot Foundation, ECTRIMS, CMSC, MEDEN, iMyoS, EMSP. B. Willekens has acted as a consultant during scientific advisory boards and/or as speaker for Alexion, Almirall, Biogen, BMS-Celgene, Galapagos, Horizon, Immunic Therapeutics, Janssen, Merck, Novartis, Roche, Sandoz, Sanofi-Genzyme. B. Willekens is member of BMS Neuroautoimmune CAR T Steering Committee. All fees were paid to UZA. B. Willekens has received research and/or patient support grants and/or sponsoring for educational events from UZA Foundation, Belgian Charcot Foundation, Start2Cure Foundation, Research Foundation (FWO) Flanders, OJO, Horlait-Dapsens Medical Foundation, EJP-RD Networking Support Scheme, Queen Elisabeth Medical Foundation, National MS Society USA, MS Liga Vlaanderen, Amgen, Biogen, Janssen, Sanofi-Genzyme, Novartis, Merck, Roche. All funds/grants were paid to UZA Foundation, UZA or UA. None of these interests are related to this study. C.S. received speaker honoraria and scientific advisory board fees from Orphalan, Servier and GlaxoSmithKline. J.B. declares no competing interests. R.L. has received grant support from Roche, Population Bio and CourPharma and has received consulting compensation and speaker honoraria from Biogen, Sanofi-Genzyme, Merck-Serono, Novartis and Hikma. M.F. declares no competing interests. F.P. received research funding from German Ministry for Education and Research (BMBF), the DFG, EU Horizon, IHI/IMI, and various public and private foundations, and research support, speaker honoraria, and personal compensation for serving on steering committees and advisory boards from Amgen, Alexion, AptaTherapeutics, Biogen, Merck, Novartis, Teva, Toleris, and UCB; he serves on the Editorial

Board of the EPMA Journal. G.M.z.H. received speaker honoraria from Argenx, Amgen, Alexion, LFB, and JnJ, compensation for serving on advisory boards from Argenx, JnJ, Roche, and Immunovant, and research funding from Novartis, Biogen, the BMBF and the DFG. C.O. declares no competing interests. J.D. received honoraria for lectures and advisory activities within the last 3 years from Alexion, Bayer, Biogen, Bristol Myers Squibb, Doctorflix, Hexal, Janssen, Juvise, Merck, Neuraxpharm, Novartis, Roche, Sanofi, and Teva. M.R. received speaker honoraria from Novartis, Bayer Vital, Roche, Alexion, Horizon/Amgen, and Ipsen, and travel reimbursement from Bayer Schering, Biogen Idec, Merz, Genzyme, Teva, Roche, Alexion, Horizon/Amgen, and Merck, none related to this study. J.K. declares no competing interests. H.S.R. is an employee of Adaptive Biotechnologies and receives salary, stock, and options as part of their employment compensation outside of the submitted work. G.L. has received compensation for lectures, advisory boards and conference participation from Alexion, Amgen, Biogen, BMS, Merck, Novartis, Roche, Sanofi. L. Klotz received compensation for serving on scientific advisory boards for Alexion, Genzyme, Janssen, Merck Serono, Novartis, and Roche, speaker honoraria and travel support from Bayer, Biogen, Genzyme, Grifols, Merck Serono, Novartis, Roche, Santhera, and Teva, and research support from the DFG, the BMBF, the Interdisciplinary Center for Clinical Studies (IZKF) Münster, IMF Münster, Biogen, Novartis, and Merck Serono. S.G.M. receives honoraria for lecturing and travel expenses for attending meetings from Academy 2, Argenx, Alexion, Almirall, Amicus Therapeutics Germany, Bayer Health Care, Biogen, BioNTech, BMS, Celgene, Datamed, Demecan, Desitin, Diamed, Diaplan, DIU Dresden, DPmed, Gen Medicine and Healthcare Products, Genzyme, Hexal, IGES, Impulze, Janssen Cilag, KW Medipoint, MedDay Pharmaceuticals, Medudy, Merck Serono, MICE, Mylan, Neuraxpharm, Neuropoint, Novartis, Novo Nordisk, ONO Pharma, Oxford PharmaGenesis, QuintilesIMS, Roche, Sanofi-Aventis, Springer Medizin Verlag, STADA, Chugai Pharma, Teva, UCB, Viatris, Wings for Life International, and Xcenda; his research is funded by the BMBF, Bundesinstitut für Risikobewertung (BfR), the DFG, the Else Kröner Fresenius Foundation, the Gemeinsamer Bundesausschuss (G-BA), the German Academic Exchange Service, the Hertie Foundation, the IZKF Münster, the German Foundation Neurology, and Alexion, Almirall, Amicus Therapeutics Germany, Biogen, Diamed, DGM e.V., Fresenius Medical Care, Genzyme, Gesellschaft von Freunden und Förderern der Heinrich-Heine-Universität Düsseldorf e.V., HERZ Burgdorf, Merck Serono, Novartis, ONO Pharma, Roche, and Teva. H.W. reported consulting fees from Biogen, Merck, Novartis, Sanofi, Genzyme, UCB, Roche, Samsung, Bristol-Myers Squibb, Alexion, Argenx, Immunic, Janssen, LTS, Lundbeck, Medix Europa, Muna Therapeutics, Myrobalan Therapeutics, Peervoice, PSL Group Services, Red Nucleus, Sangamo, Syneos, Toleranzia, Viatris, Teladoc, and the Swiss Multiple Sclerosis Society; travel support from Biogen, Merck, Sanofi, Novartis, Teva, Springer, Streamed Up, EPG Health, WebMD Health, and Ology Medical Education; participation on advisory boards for Biogen, Roche, Novartis, Merck, Genzyme, Argenx, Galapagos, UniQURE, Sandoz, and Janssen Pharmaceuticals; he serves as an expert advisor for Biogen, Roche, Novartis, Merck, Genzyme, Argenx, Galapagos, UniQURE, Sandoz, and Janssen Pharmaceuticals, all outside of the submitted work. I.K. received travel expenses for attending meetings from Pfizer, CSL Behring, and the PRESTIGE study group, and speaker honoraria from Daiichi Sankyo and Pfizer. C.C.G. received speaker honoraria from DIU Dresden AG and Kath. Klinikum Bochum, travel costs from DGN and DGLN e.V., and research funding from Biogen, Roche, and Sanofi. Adaptive Biotechnologies holds intellectual property relating to the

immunoSEQ assay and to TCR-based exposure classification, including the ECOcluster method used in this study.

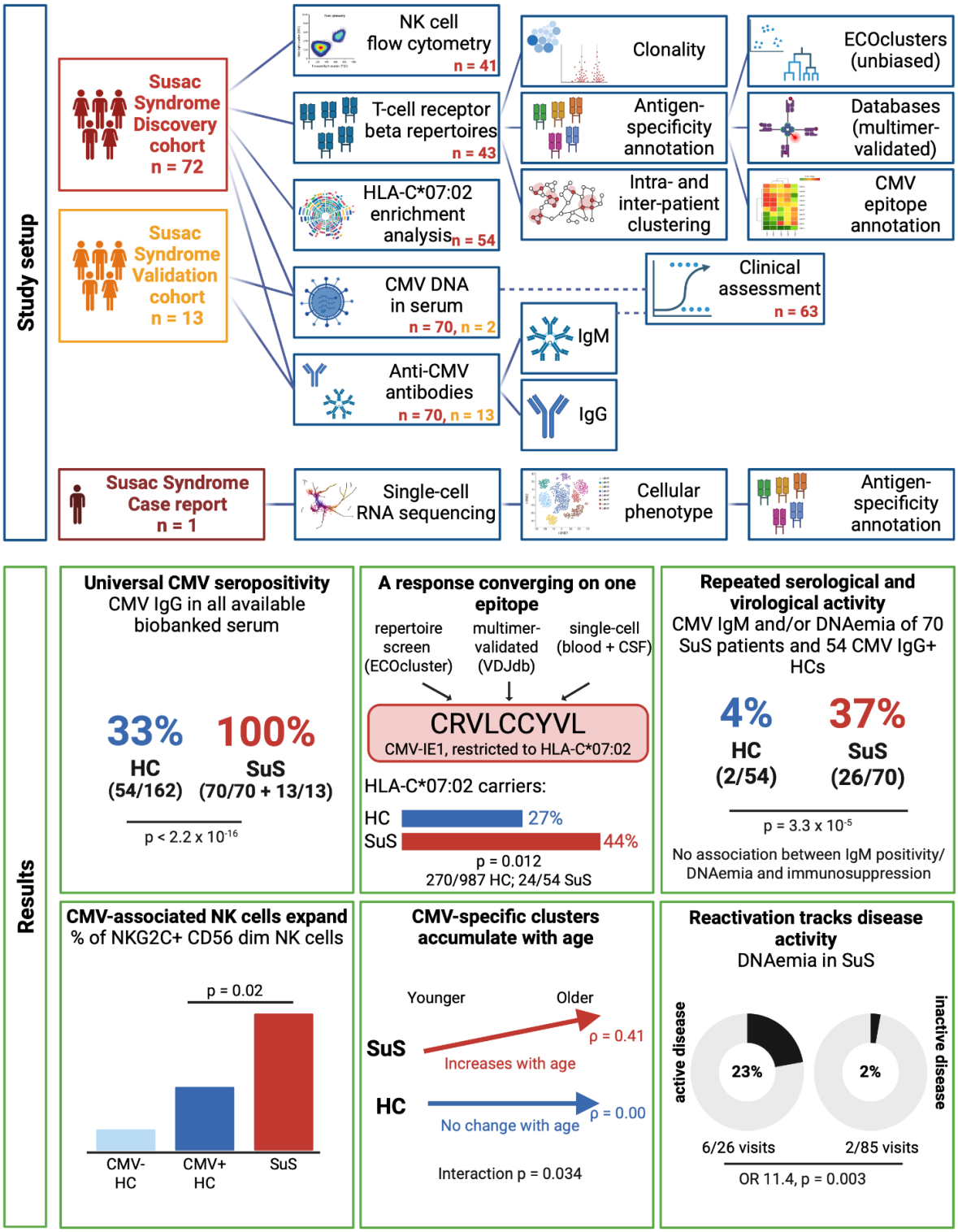
Universal seropositivity, markers of recurrent reactivation, and a convergent T-cell response implicate cytomegalovirus in Susac syndrome

Nicholas Schwab[1,*], Eva Dawin[1,*], Tilman Schneider-Hohendorf[1,*], Andreas Schulte-Mecklenbeck[2,*], Markus Kraemer[3,4], Damon May[5], Christian Wünsch[1], Simon Falk[1], Jingyun Li[1], Lukas Kaufmann[6], Antonios Katsounas[7], Eva M. Schumann[1], Steven Woodhouse[5], Bryan Howie[5], Mark Klinger[5], Edward J Osborne[5], Jennifer Moy[5], Bernhard Schlüter[8], Todd A. Hardy[9], Dimitri Hemelsoet[10], Mariano Marrodan[11], Sven Jarius[12], Klemens Ruprecht[12], Brigitte Wildemann[12], Beatrijs Wokke[13], Adi Wilf-Yarkoni[14], Barbara Willekens[15], Corinna Seliger[16], Jan Bauer[17], Roland Liblau[18], Manfred Fobker[8], Friedemann Paul[19,20], Gerd Meyer zu Hörste[1], Carolin Otto[19], Jan Dörr[20], Marius Ringelstein[4,21], Joachim Kühn[6], Harlan S. Robins[5], Guy Laureys[10], Luisa Klotz[1], Sven G. Meuth[1,§], Heinz Wiendl[2,§], Ilka Kleffner[16,§], and Catharina C. Gross[1,§]

1. Body and Brain Institute Münster, Department of Neurology, University Hospital Münster, Münster, Germany
2. Department of Neurology, University Hospital Freiburg, Freiburg, Germany
3. Department of Neurology, Alfried Krupp Krankenhaus, Essen, Germany
4. Department of Neurology, Medical Faculty and University Hospital, Heinrich Heine University Düsseldorf, Düsseldorf, Germany
5. Adaptive Biotechnologies, Seattle, WA, USA
6. Institute of Virology, University Hospital Münster, Münster, Germany
7. Department of Medicine, Knappschaft Kliniken University Hospital Bochum, Ruhr University Bochum, Bochum, Germany
8. UKM-Laboratory, University Hospital Münster, Münster, Germany
9. Department of Neurology, Concord Hospital, University of Sydney, Sydney, Australia
10. Department of Neurology, University Hospital Ghent, Ghent, Belgium
11. Neurology Department, Fleni, Buenos Aires, Argentina
12. Division of Neuroimmunology, Department of Neurology, University of Heidelberg, Heidelberg, Germany
13. Department of Neurology, MS Center ErasMS, Erasmus MC, University Medical Center, Rotterdam, The Netherlands
14. Department of Neurology, Rabin Medical Center, Petah Tikva, Israel
15. Translational Neurosciences, Laboratory for Experimental Hematology, University of Antwerp and Department of Neurology, Antwerp University Hospital, Antwerp, Belgium
16. Department of Neurology, Knappschaft Kliniken University Hospital Bochum, Ruhr University Bochum, Bochum, Germany
17. Department of Neuroimmunology, Medical University Vienna, Vienna, Austria
18. University of Toulouse, Infinity, Inserm, CNRS, Toulouse, France
19. Department of Neurology and Experimental Neurology, Charité-Universitätsmedizin Berlin, Corporate Member of Freie Universität Berlin and Humboldt-Universität zu Berlin, Berlin, Germany
20. Experimental and Clinical Research Center (ECRC) - Universitätsmedizin Berlin and Max Delbrück Center (MDC) for Molecular Medicine, Berlin, Germany
21. Center for Neurology, Department of Neuroimmunology and Neuromuscular Diseases, University Hospital and University Bonn, Bonn, Germany

*These authors contributed equally; §These authors co-supervised the study

Correspondence to: Nicholas.Schwab@ukmuenster.de; Catharina.Gross@ukmuenster.de


Study setup
Susac Syndrome Discovery cohort n = 72
Susac Syndrome Validation cohort n = 13
Susac Syndrome Case report n = 1
NK cell flow cytometry n = 41
T-cell receptor beta repertoires n = 43
HLA-C*07:02 enrichment analysis n = 54
CMV DNA in serum n = 70, n = 2
Anti-CMV antibodies n = 70, n = 13
Single-cell RNA sequencing
Clonality
Antigen-specificity annotation
Intra- and inter-patient clustering
Cellular phenotype
IgM
IgG
Clinical assessment n = 63
ECOclusters (unbiased)
Databases (multimer-validated)
CMV epitope annotation
Antigen-specificity annotation
Results
Universal CMV seropositivity
CMV IgG in all available biobanked serum
33%
HC (54/162)
100%
SuS (70/70 + 13/13)
p < 2.2 x 10-16
A response converging on one epitope
repertoire screen (ECOcluster)
multimer-validated (VDJdb)
single-cell (blood + CSF)
CRVLCCYVL
CMV-IE1, restricted to HLA-C*07:02
HLA-C*07:02 carriers:
HC 27%
SuS 44%
p = 0.012
270/987 HC; 24/54 SuS
Repeated serological and virological activity
CMV IgM and/or DNAemia of 70 SuS patients and 54 CMV IgG+ HCs
4%
HC (2/54)
37%
SuS (26/70)
p = 3.3 x 10-5
No association between IgM positivity/ DNAemia and immunosuppression
CMV-associated NK cells expand
% of NKG2C+ CD56 dim NK cells
p = 0.02
CMV- HC
CMV+ HC
SuS
CMV-specific clusters accumulate with age
Younger
Older
SuS
ρ = 0.41
Increases with age
HC
ρ = 0.00
No change with age
Interaction p = 0.034
Reactivation tracks disease activity
DNAemia in SuS
active disease
inactive disease
23%
2%
6/26 visits
2/85 visits
OR 11.4, p = 0.003

Abstract

Susac syndrome (SuS) is a rare brain, retina, and inner ear endotheliopathy, in which $CD8^+$ T cells are thought to target the microvascular endothelium. We applied unbiased, HLA-restricted antigen-specificity annotation of T-cell receptor beta-chain repertoires, followed by targeted serology, virology, and single-cell profiling, to a multicenter German cohort of 72 patients with definite SuS. Repertoires showed increased clonality and convergent expansion of CMV-specific clusters positively associated with age, alongside expansion of adaptive $NKG2C^+$ natural killer cells. T cells converged on the immediate-early-1 epitope CRVLCCYVL in carriers of HLA-C*07:02, an allele nominally enriched in this cohort, together indicating recurrent antigen exposure. Every tested patient with SuS was CMV IgG-positive (70 of 70), and 37% of patients were CMV IgM-positive or DNAemic at one or more time points. This was confirmed at diagnosis in an untreated Belgian validation cohort with 100% CMV IgG-positivity (13 of 13) and 31% IgM-positivity. Serum DNAemia, but not IgM, coincided with disease activity. Single-cell profiling of a patient with SuS, hospitalized for CMV disease eleven months before disease onset, showed the same antigenic focus alongside a CMV reactivation phenotype resembling that of allogeneic transplant recipients. These findings implicate recurrent CMV reactivation in the pathogenesis of SuS, support further prospective evaluation of diagnostic CMV testing, and provide a foundation for assessment of treatment strategies combining antiviral and immunomodulatory effects.

Introduction

Susac syndrome (SuS) is a rare inflammatory microangiopathy, primarily affecting the small arterioles of the brain, retina, and inner ear[1]. The diagnosis is defined by a triad of encephalopathy, branch retinal artery occlusions, and sensorineural hearing loss[2]. Patients with all three elements are considered to have definite SuS, whereas the presence of two elements indicates probable SuS, and one element indicates possible SuS. While clinical cohorts and pre-clinical models suggest that $CD8^+$ T-cell-mediated endothelial damage is central to SuS pathogenesis[3], the specific antigenic targets remain unknown.

Recent evidence has underscored the role of viruses in the etiology of various immune disorders: EBV infection precedes the development of multiple sclerosis (MS), potentially initiating an autoimmune cascade through molecular mimicry or epitope spreading among other mechanisms[4,5]; EBV is associated with primary sclerosing cholangitis[6], and may contribute to pathology in systemic lupus erythematosus[7]. SuS shares certain epidemiological features with MS[8], and is sometimes misdiagnosed as MS. Such misdiagnoses can be potentially harmful, because it has repeatedly been shown that some MS medications, such as interferon beta, can exacerbate SuS symptoms[9]. However, while the peripheral blood anti-EBV T-cell receptor beta (TRB) repertoire is broader in MS[10], in line with increased EBV-specific T-cell responses[11,12], it is unaltered in SuS[13], arguing against EBV as the explanation for this clinical overlap.

However, prior small SuS case series have noted cytomegalovirus (CMV) activity in patients, measured as IgM or DNA in serum[14,15]. CMV is a ubiquitous beta-herpesvirus[16], characterized by lifelong latency and a propensity for opportunistic episodic reactivation[17]. It can trigger potent systemic inflammatory responses with profound $CD8^+$ T-cell expansion[18] and is notably tropic for endothelial cells[19,20], both of which are mechanisms of pathogenic relevance in SuS.

In this study, we leveraged the unbiased diagnostic potential of TRB repertoire sequencing[21,22] in combination with targeted serological and virological assessments to investigate whether a specific viral pathogen is associated with the pathogenesis of SuS.

Results

Universal CMV seropositivity and an amplified anti-CMV T-cell response in SuS

Building on previous observations of high TRB clonality indicating clonal expansions of peripheral terminally differentiated effector-memory $CD8^+$ T cells in 14 patients with SuS[3], we expanded the analysis to a cohort of German patients with definite SuS (n = 43)[2] and control groups, including healthy controls (HC, n = 203) and patients with neuroimmunological autoimmune disorders (MS, n = 1,772; aquaporin-4-antibody-positive neuromyelitis optica spectrum disorder (NMOSD)[23], n = 90; myelin oligodendrocyte glycoprotein antibody-associated disease (MOGAD), n = 64)[24] or acute infectious diseases (COVID-19, n = 1,383; tuberculosis, n = 141)[25,26]. Patients with definite SuS exhibited higher peripheral T-cell clonality than all other groups (Fig. 1A), suggesting a strong, ongoing immune response more similar to those seen in primary infectious diseases such as COVID-19 or tuberculosis than to those seen in autoimmune diseases. As sensitivity analysis, TRB clonality was modelled, adjusting for the number of unique T-cell clonotypes per sample, with the same result.

To identify the antigenic target of these expansions without prior assumptions, we used the Exposure Co-Occurrence cluster (ECOcluster) approach[27]. This approach provides an unbiased, HLA-restricted quantification of 9,975 different T-cell response clusters, calculated as the number of sequence matches per sequencing depth ("breadth"). As a positive-control validation of the analytical framework, we first asked whether ECOcluster analysis recovered the established EBV-associated TRB repertoire signal in MS. An unbiased TRB screening in patients with MS versus non-MS controls (HC, NMOSD, MOGAD) showed an amplified T-cell response to EBV in MS according to the EBV ECOcluster[6](Fig. 1B). The lower anti-SARS-CoV-2 response in MS reflects pre-pandemic MS sampling relative to some controls. Applying the thus validated approach to SuS revealed a clear CMV signal compared to non-SuS controls (HC, MS, NMOSD, MOGAD) (Fig. 1C). To evaluate whether patients with SuS show evidence of prior CMV infection, CMV IgG titers were determined retrospectively in the earliest available biobanked serum sample after diagnosis (median 1.6 years). Strikingly, all tested patients with definite SuS were CMV IgG-positive (70 of 70, 100%; 95% CI 94.9-100%) in contrast to 33.3% in age- and sex-matched HC (54 of 162; 95% CI 26.24-40.43%; Fisher's exact test: $P < 2.2e\text{-}16$; Fig. 1D). CMV seroprevalence is strongly dependent on demographic composition, especially age and has been reported as 52% in German women of child-bearing age in 2018[28]. The 33.3% measured in our HC cohort is in line with 35.5% (143 of 403) in a recent regional cohort of pregnant women with a mean age of 33 years in southern Germany (Hadjiiona et al., 2025). In two additional HC cohorts, where TRB data allowed inference of CMV IgG status[29,30], seroprevalence was 37% in northern Germany (n = 872)[6] and 47% in the USA (n = 939)[31] at the mean age of 36 of the SuS cohort (Supplementary Figure 1). Notably, 52 of the 70 patients with SuS were treatment-naïve for intravenous or subcutaneous immunoglobulins, excluding that the universal CMV IgG-positivity in these 52 patients was due to infused antibodies.

The amplified T-cell response was not only a reflection of seroprevalence. The CMV ECOcluster[30] breadth was increased in patients with SuS, even when comparing them exclusively to 104 age- and sex-matched CMV IgG-positive HC (Fig. 1E). As the ECOcluster approach is based on TRB sequence co-occurrence and serological information but has largely untested sequence specificity[30], we compared and replicated its results with those obtained using CMV-specific TRB sequences derived from HLA-restricted multimer approaches and compiled in the public VDJdb database, thereby replicating the findings[32] (Fig. 1E). A large portion of the clonality in HC was explained by differences in CMV serostatus (P = 1.5e-5; Fig. 1F), as previously reported[33]. However, even when compared to CMV IgG-positive HC, patients with SuS still showed higher TRB clonality (*P* = 1.6e-7; Fig. 1G). Together, unbiased ECOcluster, multimer-validated specificity, and serostatus-matched clonality establish an amplified CMV-specific T-cell response in SuS compared to HC with past CMV infection.

CMV epitope-specific T-cell responses in SuS are enhanced in, but not restricted to HLA-C*07:02

To assess specific targets of the anti-CMV T-cell response, HLA-restricted CMV epitope specificities, either multimer-derived epitopes from the VDJdb or CMV ECOcluster component HLA-COclusters, were queried in individual, HLA-matched, CMV IgG-positive donor groups. This analysis revealed higher breadths against several epitopes in patients with SuS compared to HLA-matched HC (8 of 41 queried specificities) (Fig. 2A). Interestingly, the most significant changes were observed for the multimer-derived CMV immediate-early protein-1 (IE1) lytic epitope CRVLCCYVL (*P* = 7.86e-5) and for the CRVLCCYVL-specific ECOcluster feature20419 (*P* = 2.41e-4), both HLA-C*07:02-restricted.

Notably, the phenotype frequency of HLA-C*07:02 in patients with definite SuS was 44% (24 of 54 patients) compared to 25% in the age-, sex-, and CMV serostatus-matched cohort of HC (26 of 104). Statistical evaluation of this phenotype frequency in a larger HC cohort with available HLA typing found an enrichment in SuS (HC: 27.4% (270 of 987); 95% CI 24.6-30.3%; SuS: 44% (24 of 54); 95% CI 30.9-58.6%; Fisher's exact test *P* = 0.012) with a higher level of significance when restricted to CMV IgG-positive HC (95 of 376; 25.3%; 95% CI 21-30%; *P* = 0.0052). To illustrate the TRB signal strength in HLA-C*07:02 carriers and non-carriers separately, the distributions against all epitope specificities were subjected to an elastic net approach with PLS-DA visualization, which showed descriptive separation in the fitted dataset in HLA-C*07:02 carriers (Fig. 2B). However, the six epitopes with significantly higher breadth outside of HLA-C*07:02 also resulted in a detectable signal in non-carriers (Fig. 2C), suggesting a strong effect within HLA-C*07:02 without complete restriction to that allele.

We next investigated whether HLA-C*07:02-carrying patients with SuS mount a disproportionate share of their increased anti-CMV response within HLA-C*07:02. After normalizing for each donor's CMV breadth to account for the overall higher response

in SuS, patients with SuS showed a within-donor shift towards HLA-C*07:02 if present in the donor (P = 0.032, Fig. 2D), but not towards HLA-B*07:02, which is in strong linkage disequilibrium with HLA-C*07:02. This was accompanied by a larger shift towards HLA class I usage in general (P = 5.8e-4; Fig. 2E), consistent with the established involvement of $CD8^+$ T cells in SuS[3].

Convergent CMV-associated T-cell signatures and serological and virological markers are consistent with recurrent CMV activity in SuS

High TRB clonality likely reflects clonal expansion of a restricted set of dominant T-cell clonotypes. In addition to clonal expansion, antigen-associated T-cell responses can be characterized by convergence of sequence-similar TRB clonotypes[34]. As an additional analytical advantage, these convergence approaches allow for the analysis of private/non-shared TRB clonotypes, if they are connected to a cluster with partial annotation by common/shared clonotypes. An example of a highly clonal peripheral TRB repertoire in a patient with SuS including a cluster of sequence-similar, mostly CMV-annotated sequences is shown in Fig. 3A. When quantifying the number of unique TRB sequences within these similarity clusters, patients with SuS presented with a higher percentage within their 1,000 most-expanded TRB clonotypes compared to CMV IgG-positive HC (P = 2.5e-5; Fig. 3B). After repeated cell division, one TRB rearrangement is present in more than one cell and patients with SuS showed higher amounts of genomic DNA templates/cells within CMV-annotated TRB clusters (P = 4e-7; Fig. 3C), indicating clonal expansion of CMV-specific clusters in SuS.

To assess whether CMV-associated repertoire features differed with age, the number of CMV-annotated clusters was correlated with age, showing stable CMV clusters after infection in HC (Spearman rho = 0.00; $P_{Spearman}$ = 0.96). In contrast, in patients with SuS, the number of CMV clusters was positively associated with age(Spearman rho = 0.41; $P_{Spearman}$ = 0.0020; $P_{Interaction\ (Diagnosis\ X\ age)}$ = 0.034) (Fig. 3D). This cross-sectional age association is compatible with cumulative or recurrent antigen exposure, although it does not demonstrate within-person accumulation over time. Between-donor convergence analysis of the top-expanded clonotypes revealed 2,776 sequence clusters, of which four clusters with similar rearrangements were significantly enriched for CMV IgG-positive HC (nominal, unadjusted P value), whereas 106 clusters were enriched for patients with SuS (4 vs 106; Fisher's exact test comparing the proportions of HC- and SuS-enriched clusters; P < 0.0001), indicating a SuS-specific anti-CMV response (Fig. 3E). Highly CMV-annotation-enriched clusters mostly existed in patients with SuS, including T-cell responses against immediate-early CMV proteins (Fig. 3E). Collectively, these features are consistent with more frequent CMV reactivations in SuS.

To independently evaluate whether the converged T-cell response reflects recurrent CMV activity, CMV IgM titers in serum were determined in all available samples. 22 of 70 (31%) patients with SuS had IgM presence at 30 of 111 visits above the cut-off of 0.7, compared to 2 of 52 (4%) CMV IgG-positive HC (Fisher's exact test: P = 1.4e-4), and IgM titers were generally higher in SuS (P = 1.3e-5; Fig. 3F). Importantly, the IgM

elevation was not mirrored by varicella-zoster virus IgM in the tested subgroup of 32 patients with definite SuS compared to CMV IgG-positive HC (n = 29; *P* = 0.62; Supplementary Figure 2) and available serum total IgM levels from 13 of 14 tested patients were within the normal range (<2.5 g/l)[35], indicating that the serological findings support CMV activity rather than a non-specific or pan-herpesvirus response.

As plasma was unavailable, serum was also assessed for CMV DNA as a direct indicator of CMV reactivation with 9 of 127 SuS visits in 8 of 70 patients being DNA-positive compared to 0 of 79 visits in 54 CMV IgG-positive HC. Because patients contributed unequal numbers of visits, these subject-level comparisons were repeated at the visit level using linear mixed-effects models with a random intercept per individual, with each marker analysis restricted to visits at which that assay was actually performed so that untested visits did not enter as negative results. Adjusted for age and sex, patients with SuS retained a higher probability of IgM positivity over the threshold (*P* = 6.9e-4), of serum DNAemia (*P* = 0.016), and of either marker being positive (*P* = 3.3e-5) than CMV IgG-positive HC (Fig. 3G). 37% of patients (26 of 70) with SuS were positive for either marker at least once.

The serological difference proved robust in two further respects. First, it extended below the diagnostic threshold: among donors whose IgM remained below the clinical cut-off of 0.7, titers were still higher in SuS than in IgG-positive HC (*P* = 0.0017; Fig. 3H), indicating a graded rather than dichotomous difference and arguing against a threshold artifact. Second, the assay behaved as expected on internal controls: within HC, IgM titers tracked CMV IgG serostatus, being higher in IgG-positive than IgG-negative individuals (*P* = 3.7e-11; Fig. 3I), supporting the expected discrimination of the assay according to CMV serostatus.

As immunosuppressive treatment can trigger CMV reactivation[36], we next asked whether the excess reactivation in SuS was iatrogenic. Among patients with SuS, visit-level generalized estimating equations modelling each marker separately found no evidence of an association between immunosuppression within the six months preceding blood draw, with the regimens used to treat SuS, and either IgM positivity (OR 0.72, 95% CI 0.31-1.65; *P* = 0.44; 124 visits, 69 patients) or DNAemia (OR 1.44, 95% CI 0.36-5.78; *P* = 0.61; 121 visits, 68 patients) (Fig. 3J). We therefore found no indication that CMV reactivation in SuS was statistically associated with treatment.

Finally, as an antibody-independent correlate of cumulative CMV antigen encounter[37], the proportion of adaptive NKG2C^{+} cells among NKG2A^{-}CD56^{dim} natural killer (NK) cells was higher in CMV IgG-positive than in IgG-negative HC (*P* = 3.5e-4) and was further increased in patients with SuS relative to CMV IgG-positive HC (*P* = 0.02; Fig. 3K; Supplementary Figure 3), providing an additional independent line of evidence alongside the TRB repertoire and serology for elevated cumulative CMV exposure in SuS.

Single-cell profiling of a patient with SuS reveals convergent CMV-specific CD8$^+$ T-cell expansion paralleling that seen in allogeneic HSCT recipients at CMV reactivation

A 59-year-old male presented with a first generalized tonic-clonic seizure, nystagmus, dizziness, right ear hearing loss, and a temporal-inferior branch retinal artery occlusion. MRI findings showed characteristic T2 lesions in the splenium of the corpus callosum and disseminated patchy contrast enhancement. CSF analysis revealed elevated protein, lactate without pleocytosis, and detectable CMV DNA. Based on the clinical triad of encephalopathy, branch retinal artery occlusions, and sensorineural hearing loss he was diagnosed with definite SuS and treated with high-dose steroids, IVIG, and mycophenolate mofetil. Despite initial stability, he suffered a relapse requiring plasma exchange and treatment with infliximab.

Notably, the patient had been hospitalized eleven months before SuS onset for CMV-triggered secondary hemophagocytic lymphohistiocytosis with kidney involvement (stage 1 acute kidney injury) and splenomegaly, among other diagnoses. Diagnostic work-up at the time included a bone marrow biopsy and chest/abdominal CT scans, which were unremarkable, and immunofixation, which revealed equivocal monoclonal bands in the IgM and IgG fractions. The patient was treated with a combination of aciclovir and valganciclovir for 12 days and doxycycline for two weeks (following a positive test for Borrelia burgdorferi IgM). High-dose prednisolone (100 mg/day) was administered, which led to a rapid subsidence of fever, a decrease in CRP levels and the resolution of Coombs negative hemolysis.

An immunological work-up performed at the time of SuS diagnosis, after eleven months without immunosuppressive therapy, recapitulated the features observed in the larger cohort: the patient, an HLA-C*07:02 carrier, was CMV IgG-positive and showed compartmentalized viral activity, reflected by CMV DNA detectable in cerebrospinal fluid (CSF) but not serum, suggesting CMV reactivation in the CNS in this patient. The patient was also negative for DNA of EBV, HHV6, HSV, and VZV and CMV IgM-negative in serum at the time of diagnosis.

Single-cell RNA and paired TCRαβ sequencing data from peripheral blood mononuclear cells (PBMC) and CSF at diagnosis were compared with data from four previously published CMV IgG-positive HC[38,39] and, to place the findings in the context of a defined and clinically confirmed reactivation event, with a previously published cohort of four allogeneic hematopoietic stem-cell transplant recipients (HSCT) sampled longitudinally across CMV reactivation (CMV-seropositive donor, reactivation [ra]; CMV-seronegative donor, primary infection [pi])[40]. The patient with SuS showed a shift from naïve towards CD8$^+$ effector-memory T cells in both periphery and CSF, mirroring the compartment shift seen in the HSCT recipients at reactivation (Fig. 4A). This shift was accounted for in large part by CMV-specific T cells, which in the patient with SuS were almost exclusively CD8$^+$ effector-memory in the periphery and constituted the dominant expanded population in the CSF[18] (Fig. 4B). The proportion of T cells

annotated as CMV-specific in the patient with SuS exceeded that of all four HC in both compartments and was in the range of HSCT recipients (CMV-seropositive donors) at the time of clinically confirmed reactivation (Fig. 4C, D).

The antigen specificity of the response distinguished the patient even more clearly from HC. Whereas CMV-specific T cells in HC and in the HSCT recipients were dominated by late-phase specificities such as pp65 or remained unresolved, the response in the patient with SuS was focused on the immediate-early protein IE-1 and, secondarily, on early (pp50) specificities, in both PBMC and CSF (Fig. 4E), recapitulating the epitope shift observed across the cohort (Fig. 2). Nearly all CMV-specific cells in the CSF belonged to clonotypes also detected in peripheral blood (Fig. 4F), suggesting that these cells were of peripheral origin rather than locally expanded. In line with the cohort-level results, the strongest clonal expansion in both periphery and CSF was directed against the HLA-C*07:02-restricted IE-1 epitope CRVLCCYVL.

This case therefore provides an illustrative temporal association with documented CMV disease preceding SuS onset by eleven months and clinical and virological activity coinciding. Importantly, SuS developed despite prior ganciclovir treatment of the preceding CMV episode which is compatible with, but does not prove, the establishment of an autoimmune component; in this single patient, treatment of the antecedent CMV disease, therefore, did not prevent later development of SuS.

Episodes with CMV DNAemia coincide with disease activity

To test whether CMV reactivation also coincides with disease activity (defined by new activity or worsening in the brain, retina, or inner ear) at the cohort level, all study visits with available CMV serology and DNAemia assessment were assembled (Fig. 5A) and modeled using a population-averaged logistic regression (generalized estimating equations, exchangeable working correlation, robust standard errors clustered on patients) to account for repeated visits per patient. Disease activity was the dependent variable, with visit-level CMV DNAemia, CMV IgM positivity, age, and sex as covariates. The analysis was restricted to visits at which both assays were performed and disease activity was documented (63 patients, 111 visits, of which 8 were DNAemia-positive, 30 IgM-positive, 26 with, and 85 without evidence of disease activity). Detectable CMV DNA in serum was associated with concurrent disease activity (OR 11.44, 95% CI 2.28-57.44; P = 3.1e-3), whereas neither IgM positivity (OR 1.40, 95% CI 0.31-6.32; P = 0.66), nor age nor sex were associated with disease activity (Fig. 5B). Of the eight DNAemia-positive visits, six occurred during active disease (6 of 26; 23%), compared with two during inactive disease (2 of 85; 2.4%). As sensitivity analyses, the two markers were modeled separately (IgM: P = 0.91; DNA: P = 7e-3) or were subjected to a binomial linear mixed model (IgM: P = 0.56; DNA: P = 6.3e-3). Given the observational, visit-level design, these data establish temporal co-occurrence rather than direction: both reactivation preceding disease activity and disease activity precipitating reactivation remain compatible with this model.

Independent validation in a Belgian cohort

CMV serology was determined as part of the routine clinical laboratory workup and available for 13 patients with definite SuS at diagnosis prior to therapy, all with active disease. All patients were IgG-positive (13 of 13; 95% CI 75.3-100%) and four of the 13 patients were also IgM-positive above the local clinical cut-off (COI > 1.0; 31%, 95% CI 9.1-61.4%). Of note, CMV seropositivity in Belgium is approximately 58% in the general population[16]. Serum CMV DNA was assessed in two patients (one positive, one negative), and CSF CMV DNA in seven patients (zero of seven positive). These findings were consistent with those in the German cohort. Notably, one of the patients had been diagnosed with acute CMV infection with thrombocytopenia and hepatic dysfunction two years before the diagnosis of SuS, echoing the index patient in the main cohort and providing an independent instance of documented CMV disease preceding SuS onset.

Discussion

In this study, SuS was associated with a systemic anti-CMV T-cell response, universal CMV seropositivity, and serological and virological evidence of CMV reactivation co-occurring with disease activity. Seropositivity alone would indicate no more than past exposure; the informative question was whether CMV remains active in these patients, and several features of our data speak to it. The $CD8^+$-dominated anti-CMV T-cell response showed high breadth, large convergent sequence clusters, reactivity against immediate-early lytic antigens, and a positive association of CMV clusters with age. CMV IgM titers were higher in patients than in CMV IgG-positive HC, both above and below the clinical cut-off. Independent of both antibody and repertoire measurements, adaptive $NKG2C^+$ NK cells, a compartment imprinted by CMV infection and expanded by repeated antigen encounters[37], were increased above the levels seen in CMV IgG-positive HC, likely reflecting cumulative exposure. Serum CMV DNAemia and IgM positivity are also consistent with viral activity in these patients and rarely detected in immunocompetent CMV IgG-positive individuals. Cross-sectional testing finds DNA in whole blood in only 0.4% of CMV IgG-positive controls[41], and longitudinal sampling typically detects it around seroconversion but not during stable latency[42]. The observation that IgM positivity and DNAemia identified largely non-overlapping patients is consistent with their differing kinetics: CMV IgM can remain detectable for weeks to months after an acute reactivation episode has resolved, and therefore reflects recent rather than concurrent viral activity, whereas DNAemia is a transient, acute-phase marker that indexes reactivation at the time of sampling. CMV IgM positivity and/or DNAemia were detected in over one third of the discovery and validation cohorts, consistent with a recurrent process captured by cross-sectional sampling. CMV DNAemia has been reported in patients with SuS at the time of diagnosis[15], and historical series describe high CMV IgM positivity at first presentation prior to treatment initiation [14]. These prior studies together with our finding that CMV activity was not associated with prior immunosuppression in the discovery cohort and that the validation cohort was untreated all argue against a purely iatrogenic source[36].

These results revise a prior conclusion from an analysis of 14 patients, where we found no CMV-associated TRB sequences among the expanded $CD8^+$ T cells and no productively CMV-infected endothelial cells in brain tissue[3]; re-sequencing at enhanced depth of 13 of those patients in the current study with updated annotation resources recovers the signal, indicating that the earlier result reflected limited depth and annotation coverage rather than absence of a response.

It is known that CMV activity can cause a variety of different diseases including some with CNS involvement. Congenital CMV infection[43,44], CMV-mediated microvascular inflammation[19,45], idiopathic CMV encephalitis[46], and CMV disease in the context of HIV or other immunosuppressed states[47,48] show some overlap with SuS pathology. However, whereas direct viral cytopathic effects have been shown in these other diseases, evidence of this is so far lacking in SuS, suggesting that an autoimmune component might play a role in SuS.

In this, the association between EBV and MS offers a close parallel: a ubiquitous herpesvirus reaching (near-)complete seropositivity in patients with a CNS autoimmune disease[4,49,50], where no productive viral replication is reliably detectable in affected tissue, similar to SuS[3]. The EBV-MS association therefore remains a comparable precedent for the complete viral seropositivity observed here, underscoring the structural resemblance between the CMV-SuS and EBV-MS associations.

A remaining question is the distinction between the driver of the pathogenic immune response and its ultimate *in situ* targets. Our data implicate CMV reactivation but do not establish the antigen-specificity of the T-cell attack on the endothelium. In our cohort, HLA-C*07:02 was enriched in SuS, positioning HLA-C*07:02 as a potential candidate genetic risk factor and HLA-C*07:02 positive patients with SuS mounted a significantly greater proportion of their anti-CMV T-cell response via that allele compared to healthy carriers. This would be consistent with the known infection of endothelial cells by CMV [19], where it can elicit $CD8^+$ T-cell memory inflation even by latent, non-productive infection[20]. In carriers of the HLA-C*07:02 allele, infected endothelium presents CMV epitopes via this allele[51], which is comparatively resistant to viral immune evasion[52]. The pathogenic T cells may recognize CMV antigens presented on abortively infected or antigen-bearing endothelium[53], consistent with the HLA-C*07:02-focused response and the immediate-early-directed clusters observed, or the response may have broadened via molecular mimicry or epitope spreading toward an unidentified self-antigen expressed on the barrier endothelium of the brain, retina, and inner ear. The latter scenario again parallels one of the currently proposed scenarios in MS, in which EBV epitopes, largely from EBNA-1, cross-react with CNS proteins such as Anoctamin-2[54] and GlialCAM[5], a form of mimicry attributed to the lifelong latency of EBV in B cells[55,56]. The restricted tissue tropism and the immune-mediated character of the injury suggest that an autoimmune component may sustain chronic tissue damage, even while CMV activity is strongly implicated in the development and perpetuation of SuS.

An additional observation from the literature is that among 33 described patients with SuS, who had children, 21 were first diagnosed during pregnancy or the postpartum period[57], during which CMV shedding in IgG-positive women is common[58]. Although these observations derive from unsystematic case reports and are subject to ascertainment bias, they are compatible with the reactivation hypothesis. A recent study linking acute COVID-19 with reactivation of other viruses such as CMV[59] is also very much in line with several case reports of development of SuS after vaccination against SARS-CoV-2 or development of acute COVID-19[60–65].

Overall, these findings carry potential clinical implications. First, no patient with definite SuS in either cohort was CMV IgG-negative and none exist in the literature; if this holds prospectively, a negative CMV serology would argue against SuS diagnosis. Second, in one of the two patients for whom pre-onset information was available, SuS developed despite antiviral treatment of the antecedent CMV episode. A combined

antiviral and immunomodulatory approach could therefore be tested prospectively, potentially using agents with dual activity already approved for treatment of neuroinflammatory disease, such as teriflunomide or leflunomide[66,67]. Without this prospective evaluation, our findings do not yet support empirical antiviral therapy in SuS. A causal or active role of CMV remains unproven, treatment-selection criteria are lacking, and uncontrolled treatment responses would be difficult to interpret in the context of the fluctuating disease course and concomitant immunomodulatory therapy. Finally, our findings may offer a partial mechanistic rationale for the reported efficacy of IVIG in SuS[68,69], given its known anti-CMV activity[70]; whether CMV-specific IVIG confers additional benefit[71] is an open question.

One limitation of our study is that all patients were assessed after symptom onset and, therefore, a definite claim of causation is precluded. In principle, SuS could increase susceptibility to CMV, producing these associations through reverse causation. However, such a scenario is difficult to reconcile with universal seropositivity or the strong association of CMV-specific T-cell clusters with age in patients with SuS. Furthermore, two patients were hospitalized for two separate CMV diseases up to two years before diagnosis with SuS. The most probable sequence is therefore infection followed by the subsequent development of SuS symptoms, although this requires formal demonstration in a longitudinal cohort. Additionally, CMV PCR was performed on serum rather than plasma. Because serum may yield lower CMV DNA concentrations than paired plasma, negative serum PCR results may underestimate low-level DNAemia.

Taken together, beyond complete CMV IgG-positivity in 83 patients tested across two geographically separate cohorts, five converging lines of evidence implicate recurrent CMV activity due to a poorly controlled infection in the pathogenesis of SuS: CMV IgM-positivity in nearly one third of both cohorts and presence of CMV DNAemia, a clonally expanded anti-CMV T-cell response converging on an HLA-C*07:02-restricted immediate-early epitope, anti-CMV T-cell clusters with a strong positive association with age, expansion of CMV-associated NK cells, and serum DNAemia coinciding with clinical disease activity. Future research should determine, in which capacity CMV serostatus could be incorporated into the diagnostic criteria and whether antiviral strategies offer therapeutic value.

Methods

Study cohorts

The discovery cohort consisted of 72 patients with a definite SuS diagnosis[2], who were recruited between 2014 and 2026 in five German neurology clinics (Bochum, Essen, Düsseldorf, Berlin, Münster). CMV serostatus was not a factor in the diagnosis or recruitment of these patients. TRB sequencing was performed for 43 patients, HLA typing for 54 patients, and serological and virological assessments for 70 patients (Supplementary Table 1; Supplementary Figure 4) with available serum samples across 130 time points. Patient and sample numbers varied between experiments according to sample availability at the respective experimental time points. Evidence of disease activity was characterized by new hyperfluorescence or branch retinal artery occlusions on fluorescence angiography and/or new-onset or worsening sensorineural hearing loss on the audiogram and/or new cerebral lesions (including leptomeningeal contrast enhancement) on MRI independent from clinical symptoms.

Immunosuppressive exposure was coded per visit as a binary variable, indicating whether a patient had received any immunosuppressive or immunomodulatory therapy (corticosteroids including pulse therapy, mycophenolate mofetil, azathioprine, cyclophosphamide, infliximab) at any point within the six months preceding the blood draw, irrespective of whether treatment was still ongoing at the time of sampling.

The validation cohort was gathered in a single center in Belgium and consisted of 13 patients diagnosed with definite SuS, where CMV IgG and IgM, as well as CMV PCR from serum and CSF were performed for diagnostic purposes at diagnosis from fresh biomaterials before initiation of treatment.

Serological assessment

CMV IgG and IgM antibody status and titers were determined in all available biobanked samples by electrochemiluminescence immunoassay in a blinded fashion using the Elecsys IgG and IgM kits on a Cobas e801 analyzer according to the manufacturer’s instructions (Roche Diagnostics, Rotkreuz, Switzerland).

DNAemia assessment

Detection of CMV DNA in serum was performed on all available biobanked samples by polymerase chain reaction using the AltoStar® CMV PCR Kit 1.5 in a blinded fashion (altona Diagnostics, Hamburg, Germany) according to the manufacturer's instructions. Serum samples were used because plasma samples were unavailable; the use of serum was validated with serum and plasma samples from CMV DNA-positive transplant patients[72,73]. CMV DNA-positive samples were retested and rated as positive only if both results were positive. Individuals with DNA levels near the level of detection may be missed by this definition.

HLA typing

High-resolution HLA typing was performed at the DKMS Life Science Lab, accredited by European Federation of Immunogenetics and American Society for Histocompatibility and Immunogenetics. Exons 2 and 3 of HLA-A, HLA-B, HLA-C, and HLA-DRB1 were sequenced by NGS.

TRB sequencing

TRB sequencing was conducted from genomic DNA (gDNA) extracted from 10 million cryopreserved PBMC using the immunoSEQ assay (Adaptive Biotechnologies, Seattle/WA, USA). Control cohorts for the TRB clonality analysis (Fig. 1A), assessed with the same assay, were taken from previously published studies[10,13,25,26,29].

Flow cytometry

Cryopreserved PBMC were thawed and stained for spectral flow cytometry on a Cytek Aurora (Cytek Biosciences, Fremont/CA, USA) cytometer as previously described[38] using antibodies against the following antigens: CD56 (BUV737), NKG2A (CD159a; BUV615), NKG2C (CD159c; BUV395) (BD Biosciences, San Jose/CA, USA), CD16 (PE-AF700) and live/dead staining (Live/Dead Blue) (Thermo Fisher, Waltham/MA, USA). Spectral flow cytometry data were then analyzed using FlowJo software (V10.10, Becton Dickinson, Franklin Lakes/NJ, USA). The frequency of $NKG2C^{+}$ cells among $CD56^{dim}$ $NKG2A^{-}$ NK cells was quantified according to the gating strategy shown in Supplementary Figure 3.

Bioinformatic analysis

ECOcluster-based analysis

ECOclusters were defined as previously described[27]. Briefly, we computationally HLA-typed a large cohort of TRB repertoires, using high-precision HLA models[33]. We then statistically associated “public” TRBs (occurring in many donors) with specific HLAs. Within the context of an individual HLA, *h*, we clustered TRBs associated with *h* according to their patterns of occurrence within donors inferred to have *h.* We call the resulting HLA-restricted clusters HLA-COclusters. We then built cross-HLA clusters of co-occurring HLA-COclusters, termed ECOclusters. To associate a given ECOcluster with a putative exposure such as a viral infection, we performed one-sided Mann-Whitney U (MWU) tests of repertoire “breadth” on the ECOcluster (defined below) against serological labels in independent cohorts, to assess enrichment of cluster TRBs in cases over controls. We validated the specificity of these ECOcluster-label associations in holdout cohorts.

For a given HLA-COcluster *i* associated with HLA *h*, and a given TRB repertoire *r* inferred to have *h*, we define the HLA-COcluster *CR count*, CR_{ir}, as the number of unique TRB nucleotide rearrangements matching TRBs in *i* observed in TRB repertoire *r*.

We define the *HLA-COcluster breadth* HB_{ir} as CR_{ir} / UPR_r, where UPR_r is the total number of unique productive (in-frame, no stop codon) TRB nucleotide rearrangements observed in the TRB repertoire *r*.

Similarly, we define *HLA-COcluster depth* HD_{ir} as the sum of the productive frequencies of TRB nucleotide rearrangements in *r* matching TRBs in *i.* The *productive frequency* of a specific nucleotide rearrangement in repertoire *r* is the summed template count for that rearrangement, divided by the total template count of all productive rearrangements in *r*.

Then, for a given ECOcluster *e* with component HLA-COclusters $\{j_1, j_2, \ldots, j_N\}$, we can define the *ECOcluster breadth* EB_{er} as $\Sigma_{k=1}^{N} HB_{jk,r}$, and *ECOcluster depth* ED_{er} as $\Sigma_{k=1}^{N} HD_{jk,r}$.

TRB sequence matching

Database entries from VDJdb or the CMV ECOcluster were matched in TRB repertoires by CDR3 amino acid sequence and TRB chain variable gene. From VDJdb, only entries derived from multimer experiments were used, and only matches in donors with the correct HLA background of the annotated entry were counted. Breadth was calculated by adding all unique productive rearrangements in a sample matched to CMV or a specific epitope and dividing by the number of rearrangements in that sample. Depth was calculated by adding the productive frequency of these matched rearrangements in a sample.

Productive clonality

Productive clonality was calculated as the square root of Simpson's index (Σp_i^2), where p_i is the proportional abundance of each unique productive TRB nucleotide rearrangement.

Epitope quantification

Sequence matching was performed in HLA-eligible donors as described above. Breadth was then statistically assessed using either linear models (for VDJdb epitopes, which in theory could include TRB entries for more than one HLA allele) or Wilcoxon tests in donors with one common HLA allele (for HLA-COclusters that are by definition HLA-restricted to one allele).

Elastic net analysis

To test whether donor-level patterns of HLA-restricted CMV-specificities discriminate SuS from CMV IgG-positive HC, an elastic-net logistic regression classifier was trained on the matrix of per-donor breadth values across all queried VDJdb epitopes and CMV ECOcluster component HLA-COclusters. Features with fewer than two non-zero observations across donors were excluded; remaining features were internally standardized. The classifier was fitted separately in HLA-C*07:02 carriers and non-carriers. Within each stratum, performance was estimated by leave-one-out cross-

validation: for each held-out donor, the regularization parameter λ was selected by inner 3-5-fold cross-validation (class-balanced folds, λ at minimum binomial deviance), and the mixing parameter α was chosen from a grid {0.1, 0.5, 1.0}. The α selected by majority vote across LOOCV iterations was then used to re-fit a final model on all donors in the stratum for feature extraction. Classifier performance was reported as the area under the receiver-operating curve with 95% DeLong confidence intervals and operating thresholds were derived by Youden's J. Elastic-net-selected features were further visualized by partial least-squares discriminant analysis (PLS-DA) within each stratum, with two latent variables, per-feature scaling, and leave-one-out classification accuracy estimated by the maximum-distance prediction rule; the sign of latent variable 1 was oriented such that patients with SuS lay on its positive side, an operation that does not affect classification.

Intra-individual TRB similarity clustering

For the top 1,000 most prevalent TRB rearrangements in a repertoire, a TCRdist matrix was constructed[74]; rearrangements separated by a distance threshold of 12 or less (approximately equivalent to a Hamming distance of 1, but better suited for TRB sequences) were considered to be part of one cluster.

Phase annotation

CMV epitopes were grouped into immediate-early, early, and late phases of the lytic anti-CMV response[18]. In the case of HLA-COclusters, MIRA data[75] were used (Supplementary Table 2), where available, to find the feature's most probable epitope. In several cases, there was sequence overlap between ECOclusters and VDJdb entries (*e.g.*, VDJdb epitope CRVLCCYVL and HLA-COcluster feature20419 or the epitope VTEHDTLLY and feature339), which allowed us to cross-validate the epitope restriction suggested by MIRA.

Inter-individual TRB similarity clustering

For the top 1,000 most prevalent TRB rearrangements of all repertoires in the analysis, a TCRdist matrix[74] was constructed, and DBSCAN[76] was used with an $\varepsilon = 12$ and a minimum cluster size of three sequences. Clusters were then assessed for statistical enrichment of either HC or patients with SuS at the donor level using Fisher's exact test of donors in a cluster.

Single-cell RNA sequencing

Single-cell suspensions were processed using the 10x Genomics Chromium Next GEM Single Cell 5' platform (10x Genomics, Pleasanton/CA, USA). Cells were partitioned into gel bead-in-emulsion and barcoded according to the standard 10x Genomics 5' protocol. Gene-expression libraries together with paired V(D)J immune repertoire (TCR and BCR) libraries were prepared from the same captured cells. Libraries were sequenced on an Illumina platform (Illumina, San Diego/CA, USA). Raw sequencing reads were processed with Cell Ranger (v8.0.1, 10x Genomics) using the cellranger multi pipeline, jointly aligning gene-expression and V(D)J data per sample.

Reads were aligned to the GRCh38 human reference (refdata-gex-GRCh38-2024-A) for gene expression and to the corresponding Cell Ranger V(D)J reference (GRCh38, Ensembl 7.1.0) for TCR and BCR assembly. Cell calling, barcode and UMI counting, and clonotype assembly were performed with default parameters, yielding filtered feature-barcode matrices and contig annotations for downstream analysis. Sample-level HLA genotypes were inferred directly from the single-cell gene-expression reads using arcasHLA[77], which extracts and re-aligns reads mapping to the HLA region to predict class I and class II allele genotypes at high resolution. In samples with unavailable serostatus, CMV serostatus was inferred with CMVerify[78], a machine-learning tool that predicts CMV serostatus from single-cell gene-expression data. As additional positive controls, one CMV IgG-positive sample from a previously published study [38] and three from a second published study[39] were included. The latter study was financially supported by the National Institutes of Health and downloaded from the National Institutes of Health's dbGaP database (accession phs002222.v2.p1).

Single-cell sequencing data integration and clustering

Filtered feature-barcode matrices from the cohorts described above, together with an external longitudinal cytomegalovirus (CMV)-reactivation kinetics cohort [40] and pre-computed Azimuth reference cell-type predictions, were merged into a single SingleCellExperiment object (236,095 cells x 20,022 genes across 33 samples spanning four cohorts) prior to reprocessing. Per-cell quality-control metrics (total UMI count, number of detected genes, and percentage of counts mapping to mitochondrial and ribosomal gene sets) were computed with scater::perCellQCMetrics (scater v1.38.0). Outlier cells were flagged per sample using scran::isOutlier (scran v1.38.0) at a threshold of 3 median absolute deviations from the per-sample median (low tail for library size and detected-gene count, high tail for mitochondrial percentage), supplemented by an absolute floor (library size < 500 UMIs, detected genes < 200, or mitochondrial fraction > 20%). Heterotypic doublets were identified with scDblFinder (v1.24.0). Cells failing either criterion were excluded (21,312 cells, 9.03% of input), yielding a filtered dataset of 214,783 cells x 19,917 genes.

Highly variable genes were identified from the library-size-normalized, log-transformed expression matrix by modeling the mean-variance trend with scran::modelGeneVar, blocking on study of origin to limit selection of genes driven by inter-cohort technical variation; the top 2,500 genes by biological-component rank were retained for principal component analysis (PCA; scater::runPCA, 50 components, randomized SVD). Batch effects across the 33 samples were corrected by applying Harmony (harmony v2.0.5)[79], and applied to the 50-dimensional PCA embedding with sample identity as the integration variable; Harmony converged after 5 iterations. Uniform manifold approximation and projection (UMAP; scater::runUMAP, 30 dimensions) was computed on the Harmony-corrected embedding for visualization and downstream figure generation.

Cell-type proportions were compared among donors by computing per-sample cell-type fractions stratified by tissue (CSF, PBMC); given the single-patient design, this

analysis is descriptive and reported as exploratory. All integration and clustering analyses were performed in R (v4.5.3).

Statistics

Statistical tests are reported in the figure legends. Generally, non-parametric tests were performed (Mann-Whitney tests, Spearman correlations). Fisher's exact tests were used to assess binary distributions (*e.g.* donor distributions in clusters or antibody/DNA positivity). If many hypotheses were tested (Fig. 1B, Fig. 1C, and Fig. 2A), *P* value adjustment using Benjamini-Hochberg [80] was applied.

Visit-level modelling of CMV reactivation markers

Because patients contributed unequal numbers of longitudinal samples, subject-level comparisons of reactivation markers were complemented by models fitted at the level of the individual study visit, which retain all sampling time points while accounting for the non-independence of repeated measurements within a donor.

Marker positivity was defined only for visits at which the corresponding assay was actually performed. Visits without a given assay were treated as missing for that marker and excluded from the corresponding model, rather than being counted as negative results; each marker model was therefore fitted to its own analysis set, and models including both markers simultaneously were restricted to complete cases. Sample sizes for each model (number of visits and number of contributing patients) are reported in the corresponding figure legend or results text.

Group differences in reactivation between patients with definite SuS and CMV IgG-positive HC (Fig. 3G) were estimated using linear mixed-effects models with a random intercept per individual, fitted with the lme4 and lmerTest packages in R. Binary marker status (IgM positivity above the clinical cut-off, serum CMV DNAemia, or either marker positive) was modelled as the dependent variable, with diagnostic group as the fixed effect of interest and age and sex as covariates. Coefficients are therefore interpretable as the adjusted difference in the probability of marker positivity relative to CMV IgG-positive HC. Confidence intervals were obtained by the Wald method, and P values were calculated using two-sided t-tests with Satterthwaite-approximated degrees of freedom.

Associations within the SuS cohort between immunosuppressive treatment and each reactivation marker (Fig. 3J), and between reactivation markers and concurrent clinical disease activity (Fig. 5B) were estimated using population-averaged logistic regression fitted by generalized estimating equations (geepack package in R), with an exchangeable working correlation structure and robust (sandwich) standard errors clustered on patient identifiers. These models yield marginal odds ratios with cluster-robust inference appropriate for repeated visits per patient. Age and sex were included as covariates throughout. Continuous covariates were standardized where indicated in the figure legends; odds ratios for standardized covariates are reported per standard deviation. All models were checked for convergence and for degenerate variance estimates arising from sparse cells or collapsed clustering, and no model with non-finite standard errors is reported. All modeling was performed in R (v4.5.3).

718

719

Funding

Study funding was provided by NFDI4Immuno from the German Research Foundation (DFG), grant number 501875662 to NS and single research grant 585413552 to CCG.

Study approval

All experiments and sample collections were carried out in accordance with the Declaration of Helsinki and were approved by the local ethics committee in Münster, Germany (Ethics Committee of the Board of Physicians of the Region Westfalen-Lippe (2014-068-f-S, 2016-053-f-S, 2019-712-f-S, 2024-653-f-S)) and of Ghent University hospital (2019/1443). Written informed consent was obtained from all patients prior to inclusion in the study.

Sex and gender reporting

Sex was self-reported and refers to biological attributes. Gender identity was not collected in this study, and no analyses are disaggregated by gender.

Both female and male participants were included in all cohorts. In the discovery cohort, the sex distribution (f:m) was 49:21 for serological assessment, 48:20 for CMV DNAemia assessment, and 29:14 for TRB sequencing; healthy control groups were sex-matched to the corresponding patient group (116:46, 37:14, and 68:36, respectively; all $P \geq 0.84$, Supplementary Table 1). The female predominance reflects the known sex distribution of Susac syndrome rather than a recruitment criterion; no participant was included or excluded on the basis of sex. The patient characterised by single-cell profiling was male.

Sex was included as a covariate in all visit-level models of CMV reactivation markers, of the association between immunosuppression and reactivation, and of the association between reactivation and disease activity; it was not associated with any outcome (Fig. 3J, Fig. 5B). Given the rarity of the disease and the resulting cohort size, the study was not powered for formally sex-stratified analyses, and sex-disaggregated results should be regarded as exploratory. Sex-disaggregated participant counts are provided in Supplementary Table 1.

Acknowledgements

The authors would like to thank the neurological biobank Münster, the central biobank Münster, and Barbara Meyring for technical support during the study. The authors would also like to thank all contributing patients and recruiting centers, without whom the study would not have been possible. The study overview was created using BioRender.

Data availability

The TRB repertoires of patients with SuS and healthy IgG-positive controls (Figures 2+3) as well as the previously unpublished single cell RNA sequencing data (Fig. 4) are available without restriction on Zenodo (10.5281/zenodo.22246432).

A link for the duration of the peer-review process is here:

https://zenodo.org/records/22246432?preview=1&token=eyJhbGciOiJIUzUxMiJ9.eyJpZCI6IjI5NTNjMjgxLWRhNDktNDVkZC05ZDI2LTM3YWI0NzM5MmMwNyIsImRhdGEiOnt9LCJyYW5kb20iOiIxMzgxMTcwYmVhZTdmYjRhZmViYTAxYTM1MmRmZmQ5NyJ9.sbmxbJ-O9sr4Gakvm8mGZWkSsrTF4iQg-_IJml-udafD28DWLcdiq8BwGKG61kaEuMb4o-rF1-PgLeTpBmzs3w

Author contributions

N.S., E.D., T.S.-H. and A.S.-M. contributed equally. S.G.M., H.W., I.K. and C.C.G. jointly supervised the study.

Conceptualization: N.S., T.S.-H., I.K., C.C.G.

Methodology: N.S., T.S.-H., D.M., S.W., B.H., H.S.R.

Software: D.M., S.W., B.H.

Formal analysis: N.S., T.S.-H., D.M., S.F., J.L.

Investigation: E.D., A.S.-M., C.W., S.F., L. Kaufmann, B.S., D.H., M.F., J.K., G.L.

Validation: L. Kaufmann, J.K.

Resources: M. Kraemer, A.K., E.M.S., K.R., C.S., F.P., J.D., M.R., L. Klotz, S.G.M., H.W., I.K. and C.C.G. provided patients, clinical data and biospecimens for the discovery cohort. D.H. and G.L. provided the validation cohort. S.J. and B. Wildemann provided control cohorts. M. Klinger, E.J.O., J.M. and H.S.R. provided TRB reference data and ECOcluster/MIRA resources. S.F. and G.M.z.H. provided single-cell reference data.

Data curation: N.S., E.D., E.M.S., I.K.

Visualization: N.S., T.S.-H.

Funding acquisition: N.S., C.C.G.

Project administration: N.S., C.C.G.

Supervision: N.S., J.K., G.L., L. Klotz, S.G.M., H.W., I.K., C.C.G.

Writing – original draft: N.S.

Writing – review & editing: all authors. T.A.H., M.M., B. Wokke, A.W.-Y., B. Willekens, J.B., R.L. and C.O. critically revised the manuscript for important intellectual content and contributed to the Discussion.

All authors approved the final manuscript and agree to be accountable for the work.

Competing interests

N.S. declares no competing interests. E.D. declares no competing interests. T.S.-H. declares no competing interests. A.S.-M. declares no competing interests. M. Kraemer declares no competing interests. D.M. is an employee of Adaptive Biotechnologies and receives salary, stock, and options as part of their employment compensation outside of the submitted work. C.W. declares no competing interests. S.F. declares no competing interests. J.L. declares no competing interests. L. Kaufmann declares no competing interests. A.K. declares no competing interests. E.M.S. declares no competing interests. S.W. is an employee of Adaptive Biotechnologies and receives salary, stock, and options as part of their employment compensation outside of the submitted work. B.H. is an employee of Adaptive Biotechnologies and receives salary, stock, and options as part of their employment compensation outside of the submitted work. M. Klinger is an employee of Adaptive Biotechnologies and receives salary, stock, and options as part of their employment compensation outside of the submitted work. E.J.O. is an employee of Adaptive Biotechnologies and receives salary, stock, and options as part of their employment compensation outside of the submitted work. J.M. is an employee of Adaptive Biotechnologies and receives salary, stock, and options as part of their employment compensation outside of the submitted work. B.S. declares no competing interests. T.A.H. received speaker honoraria, conference support, or scientific advisory board fees from Bayer-Schering, Bristol-Myers Squibb, Biogen-Idec, Merck, Novartis, Roche, UCB, Sanofi-Genzyme, Alexion, Sandoz, Teva, and Neuraxpharm. D.H. declares no competing interests. M.M. declares no competing interests. S.J. declares no competing interests. K.R. received research support from the European Union (821283-2), Stiftung Charité, the Guthy-Jackson Charitable Foundation, and the Arthur Arnstein Foundation, and speaker honoraria from Virion Serion and Novartis. B. Wildemann received research support from the Federal Ministry of Research, Technology and Space, the German Research Foundation (DFG), the Baden-Württemberg Ministry of Science, Research and Arts, Argenx, Novartis, and Roche, and honoraria and/or travel support from Alexion, Argenx, INSTAND, Neuraxpharm, Novartis, and Roche. B. Wokke received research support from Hansa Biopharma, none related to this study. A.W.-Y. declares no competing interests. B. Willekens received travel support to attend conferences and meetings from Biogen, Sanofi-Genzyme, Merck, Neuraxpharm, Novartis, Roche, UCB, EAN, European Charcot Foundation, ECTRIMS, CMSC, MEDEN, iMyoS, EMSP. B. Willekens has acted as a consultant during scientific advisory boards and/or as speaker for Alexion, Almirall, Biogen, BMS-Celgene, Galapagos, Horizon, Immunic Therapeutics, Janssen, Merck, Novartis, Roche, Sandoz, Sanofi-Genzyme. B.

Willekens is member of BMS Neuroautoimmune CAR T Steering Committee. All fees were paid to UZA. B. Willekens has received research and/or patient support grants and/or sponsoring for educational events from UZA Foundation, Belgian Charcot Foundation, Start2Cure Foundation, Research Foundation (FWO) Flanders, OJO, Horlait-Dapsens Medical Foundation, EJP-RD Networking Support Scheme, Queen Elisabeth Medical Foundation, National MS Society USA, MS Liga Vlaanderen, Amgen, Biogen, Janssen, Sanofi-Genzyme, Novartis, Merck, Roche. All funds/grants were paid to UZA Foundation, UZA or UA. None of these interests are related to this study. C.S. received speaker honoraria and scientific advisory board fees from Orphalan, Servier and GlaxoSmithKline. J.B. declares no competing interests. R.L. has received grant support from Roche, Population Bio and CourPharma and has received consulting compensation and speaker honoraria from Biogen, Sanofi-Genzyme, Merck-Serono, Novartis and Hikma. M.F. declares no competing interests. F.P. received research funding from German Ministry for Education and Research (BMBF), the DFG, EU Horizon, IHI/IMI, and various public and private foundations, and research support, speaker honoraria, and personal compensation for serving on steering committees and advisory boards from Amgen, Alexion, AptaTherapeutics, Biogen, Merck, Novartis, Teva, Toleris, and UCB; he serves on the Editorial Board of the EPMA Journal. G.M.z.H. received speaker honoraria from Argenx, Amgen, Alexion, LFB, and JnJ, compensation for serving on advisory boards from Argenx, JnJ, Roche, and Immunovant, and research funding from Novartis, Biogen, the BMBF and the DFG. C.O. declares no competing interests. J.D. received honoraria for lectures and advisory activities within the last 3 years from Alexion, Bayer, Biogen, Bristol Myers Squibb, Doctorflix, Hexal, Janssen, Juvise, Merck, Neuraxpharm, Novartis, Roche, Sanofi, and Teva. M.R. received speaker honoraria from Novartis, Bayer Vital, Roche, Alexion, Horizon/Amgen, and Ipsen, and travel reimbursement from Bayer Schering, Biogen Idec, Merz, Genzyme, Teva, Roche, Alexion, Horizon/Amgen, and Merck, none related to this study. J.K. declares no competing interests. H.S.R. is an employee of Adaptive Biotechnologies and receives salary, stock, and options as part of their employment compensation outside of the submitted work. G.L. has received compensation for lectures, advisory boards and conference participation from Alexion, Amgen, Biogen, BMS, Merck, Novartis, Roche, Sanofi. L. Klotz received compensation for serving on scientific advisory boards for Alexion, Genzyme, Janssen, Merck Serono, Novartis, and Roche, speaker honoraria and travel support from Bayer, Biogen, Genzyme, Grifols, Merck Serono, Novartis, Roche, Santhera, and Teva, and research support from the DFG, the BMBF, the Interdisciplinary Center for Clinical Studies (IZKF) Münster, IMF Münster, Biogen, Novartis, and Merck Serono. S.G.M. receives honoraria for lecturing and travel expenses for attending meetings from Academy 2, Argenx, Alexion, Almirall, Amicus Therapeutics Germany, Bayer Health Care, Biogen, BioNTech, BMS, Celgene, Datamed, Demecan, Desitin, Diamed, Diaplan, DIU Dresden, DPmed, Gen Medicine and Healthcare Products, Genzyme, Hexal, IGES, Impulze, Janssen Cilag, KW Medipoint, MedDay Pharmaceuticals, Medudy, Merck Serono, MICE, Mylan, Neuraxpharm, Neuropoint, Novartis, Novo Nordisk, ONO Pharma, Oxford PharmaGenesis, QuintilesIMS, Roche, Sanofi-Aventis, Springer

Medizin Verlag, STADA, Chugai Pharma, Teva, UCB, Viatris, Wings for Life International, and Xcenda; his research is funded by the BMBF, Bundesinstitut für Risikobewertung (BfR), the DFG, the Else Kröner Fresenius Foundation, the Gemeinsamer Bundesausschuss (G-BA), the German Academic Exchange Service, the Hertie Foundation, the IZKF Münster, the German Foundation Neurology, and Alexion, Almirall, Amicus Therapeutics Germany, Biogen, Diamed, DGM e.V., Fresenius Medical Care, Genzyme, Gesellschaft von Freunden und Förderern der Heinrich-Heine-Universität Düsseldorf e.V., HERZ Burgdorf, Merck Serono, Novartis, ONO Pharma, Roche, and Teva. H.W. reported consulting fees from Biogen, Merck, Novartis, Sanofi, Genzyme, UCB, Roche, Samsung, Bristol-Myers Squibb, Alexion, Argenx, Immunic, Janssen, LTS, Lundbeck, Medix Europa, Muna Therapeutics, Myrobalan Therapeutics, Peervoice, PSL Group Services, Red Nucleus, Sangamo, Syneos, Toleranzia, Viatris, Teladoc, and the Swiss Multiple Sclerosis Society; travel support from Biogen, Merck, Sanofi, Novartis, Teva, Springer, Streamed Up, EPG Health, WebMD Health, and Ology Medical Education; participation on advisory boards for Biogen, Roche, Novartis, Merck, Genzyme, Argenx, Galapagos, UniQURE, Sandoz, and Janssen Pharmaceuticals; he serves as an expert advisor for Biogen, Roche, Novartis, Merck, Genzyme, Argenx, Galapagos, UniQURE, Sandoz, and Janssen Pharmaceuticals, all outside of the submitted work. I.K. received travel expenses for attending meetings from Pfizer, CSL Behring, and the PRESTIGE study group, and speaker honoraria from Daiichi Sankyo and Pfizer. C.C.G. received speaker honoraria from DIU Dresden AG and Kath. Klinikum Bochum, travel costs from DGN and DGLN e.V., and research funding from Biogen, Roche, and Sanofi. Adaptive Biotechnologies holds intellectual property relating to the immunoSEQ assay and to TCR-based exposure classification, including the ECOcluster method used in this study.

Figures and Figure Legends

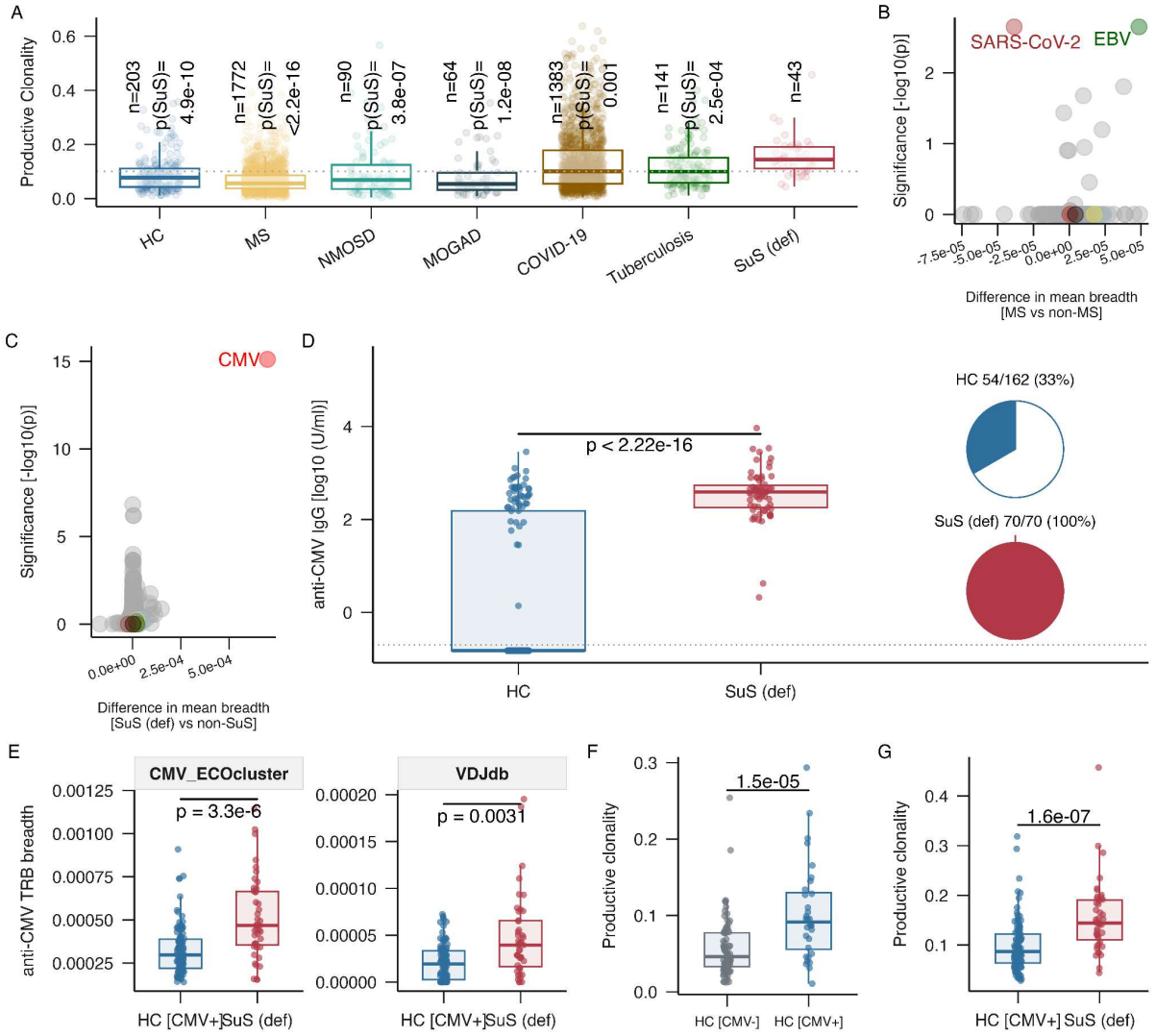


Figure 1. Universal CMV seropositivity and an amplified anti-CMV T-cell response in SuS.

(A) Productive TRB clonality in peripheral blood of healthy controls (HC, n = 203) and patients with multiple sclerosis (MS, n = 1,772), neuromyelitis optica spectrum disorder (NMOSD, n = 90), myelin oligodendrocyte glycoprotein antibody-associated disease (MOGAD, n = 64)[13], COVID-19 (n = 1,383)[26], tuberculosis (n = 141)[25], and definite Susac syndrome (SuS (def), n = 43). *P* values were determined by a two-sided Wilcoxon rank-sum test for each group versus SuS (def). Dotted line indicates a reference clonality of 0.1.

(B,C) Volcano plots comparing mean TRB repertoire "breadth" (fraction of the unique T-cell clonotypes annotated to a given TRB cluster) between **(B)** patients with MS and non-MS control cohorts (HC, n = 203, NMOSD, n = 90, MOGAD, n = 64) and **(C)** patients with SuS (def) and non-SuS control cohorts (HC, n = 203, MS, n = 1772, NMOSD, n = 90, MOGAD, n = 64). Each point represents one cluster; known

associations are colored by the annotated pathogen (CMV, HSV-1, HSV-2, parvovirus, RSV, EBV, SARS-CoV-2, toxoplasma, or unknown/unassigned). *P* values were calculated using a two-sided Mann-Whitney U test, Benjamini-Hochberg (BH)-adjusted; the most significant pathogen(s) in each comparison are labeled directly (EBV and SARS-CoV-2 in **B**; CMV in **C**).

(D) CMV IgG titers (log10 IU/ml) in HC (n = 162) and SuS (def, n = 70). *P* values were calculated using a two-sided Wilcoxon rank-sum test. Pie charts show the fraction of CMV IgG-positive donors per group (positive/total tested, %). The dotted gray line indicates the threshold for seropositivity.

(E) Anti-CMV TRB "breadth" (fraction of T-cell clonotypes annotated as CMV-specific) in CMV IgG-positive HC (HC [CMV+], n = 104) versus SuS (def, n = 43), independently derived from two reference annotation sources: Exposure Co-Occurrence clusters (CMV_ECOcluster, left) and VDJdb (right). *P* values were calculated using a two-sided Wilcoxon rank-sum test.

(F) Productive TRB clonality in HC stratified by CMV serostatus (CMV IgG-negative (n = 82) versus CMV IgG-positive (n = 32). *P* values were calculated using a two-sided Wilcoxon rank-sum test.

(G) Productive TRB clonality in CMV IgG-positive HC (HC [CMV+], n = 104) versus SuS (def, n = 43). *P* values were calculated using a two-sided Wilcoxon rank-sum test.

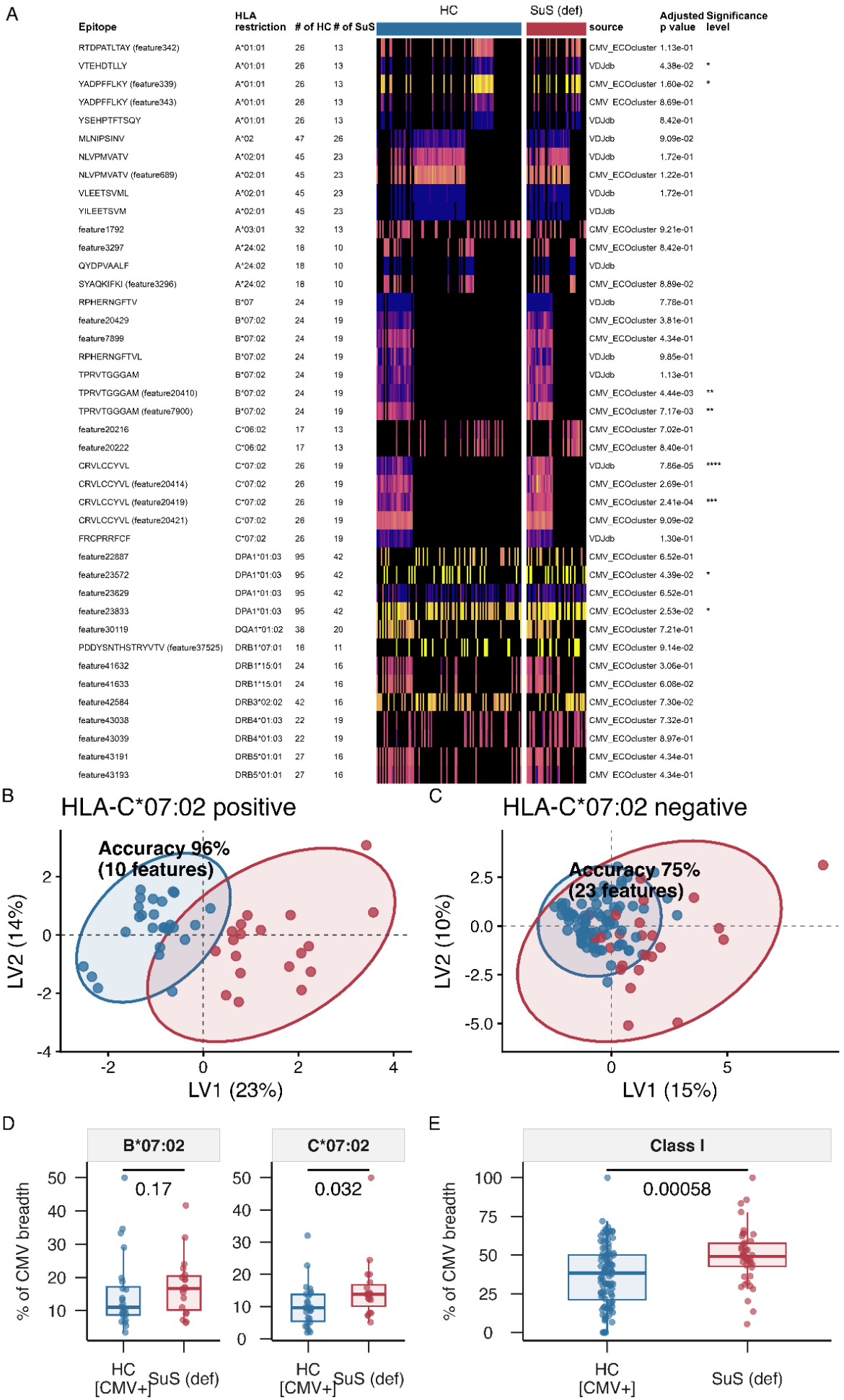

A
Epitope
HLA restriction
# of HC
# of SuS
HC
SuS (def)
source
Adjusted p value
Significance level
RTDPATLTAY (feature342) A*01:01 26 13 CMV_ECOcluster 1.13e-01
VTEHDTLLY A*01:01 26 13 VDJdb 4.38e-02 *
YADPFFLKY (feature339) A*01:01 26 13 CMV_ECOcluster 1.60e-02 *
YADPFFLKY (feature343) A*01:01 26 13 CMV_ECOcluster 8.69e-01
YSEHPTFTSQY A*01:01 26 13 VDJdb 8.42e-01
MLNIPSINV A*02 47 26 VDJdb 9.09e-02
NLVPMVATV A*02:01 45 23 VDJdb 1.72e-01
NLVPMVATV (feature689) A*02:01 45 23 CMV_ECOcluster 1.22e-01
VLEETSVML A*02:01 45 23 VDJdb 1.72e-01
YILEETSVM A*02:01 45 23 VDJdb
feature1792 A*03:01 32 13 CMV_ECOcluster 9.21e-01
feature3297 A*24:02 18 10 CMV_ECOcluster 8.42e-01
QYDPVAALF A*24:02 18 10 VDJdb
SYAQKIFKI (feature3296) A*24:02 18 10 CMV_ECOcluster 8.89e-02
RPHERNGFTV B*07 24 19 VDJdb 7.78e-01
feature20429 B*07:02 24 19 CMV_ECOcluster 3.81e-01
feature7899 B*07:02 24 19 CMV_ECOcluster 4.34e-01
RPHERNGFTVL B*07:02 24 19 VDJdb 9.85e-01
TPRVTGGGAM B*07:02 24 19 VDJdb 1.13e-01
TPRVTGGGAM (feature20410) B*07:02 24 19 CMV_ECOcluster 4.44e-03 **
TPRVTGGGAM (feature7900) B*07:02 24 19 CMV_ECOcluster 7.17e-03 **
feature20216 C*06:02 17 13 CMV_ECOcluster 7.02e-01
feature20222 C*06:02 17 13 CMV_ECOcluster 8.40e-01
CRVLCCYVL C*07:02 26 19 VDJdb 7.86e-05 ****
CRVLCCYVL (feature20414) C*07:02 26 19 CMV_ECOcluster 2.69e-01
CRVLCCYVL (feature20419) C*07:02 26 19 CMV_ECOcluster 2.41e-04 ***
CRVLCCYVL (feature20421) C*07:02 26 19 CMV_ECOcluster 9.09e-02
FRCPRRFCF C*07:02 26 19 VDJdb 1.30e-01
feature22887 DPA1*01:03 95 42 CMV_ECOcluster 6.52e-01
feature23572 DPA1*01:03 95 42 CMV_ECOcluster 4.39e-02 *
feature23829 DPA1*01:03 95 42 CMV_ECOcluster 6.52e-01
feature23833 DPA1*01:03 95 42 CMV_ECOcluster 2.53e-02 *
feature30119 DQA1*01:02 38 20 CMV_ECOcluster 7.21e-01
PDDYSNTHSTRYVTV (feature37525) DRB1*07:01 16 11 CMV_ECOcluster 9.14e-02
feature41632 DRB1*15:01 24 16 CMV_ECOcluster 3.06e-01
feature41633 DRB1*15:01 24 16 CMV_ECOcluster 6.08e-02
feature42584 DRB3*02:02 42 16 CMV_ECOcluster 7.30e-02
feature43038 DRB4*01:03 22 19 CMV_ECOcluster 7.32e-01
feature43039 DRB4*01:03 22 19 CMV_ECOcluster 8.97e-01
feature43191 DRB5*01:01 27 16 CMV_ECOcluster 4.34e-01
feature43193 DRB5*01:01 27 16 CMV_ECOcluster 4.34e-01
B
HLA-C*07:02 positive
Accuracy 96%
(10 features)
LV2 (14%)
LV1 (23%)
C
HLA-C*07:02 negative
Accuracy 75%
(23 features)
LV2 (10%)
LV1 (15%)
D
B*07:02
C*07:02
0.17
0.032
% of CMV breadth
HC [CMV+]
SuS (def)
E
Class I
0.00058
% of CMV breadth
HC [CMV+]
SuS (def)

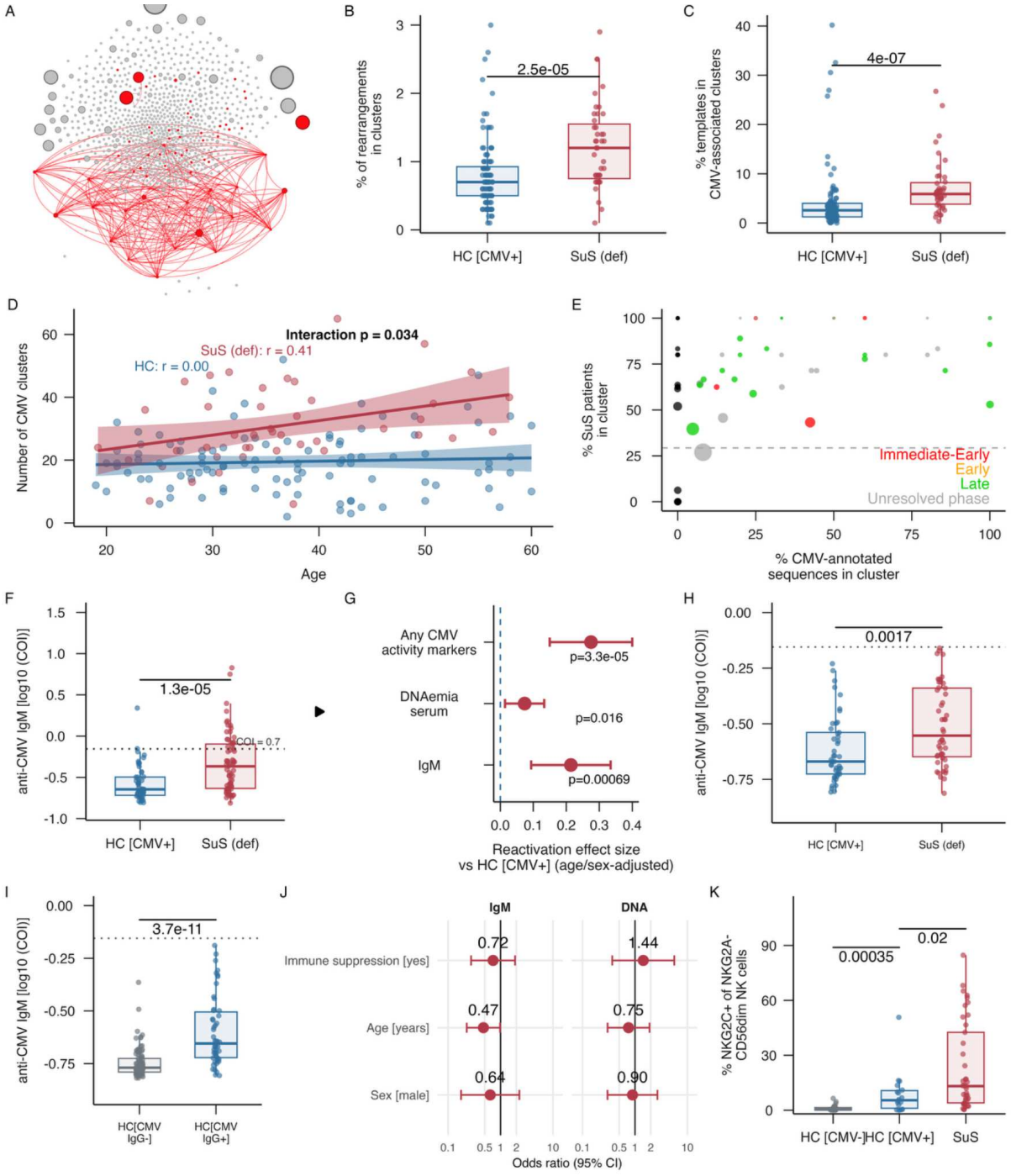
Figure 2. CMV epitope-specific T-cell responses in SuS are focused in, but not restricted to HLA-C*07:02.

(A) Heatmap of per-individual TRB binding evidence for candidate/known CMV-derived epitopes (rows), annotated with HLA restriction, the number of HC and SuS (def) donors carrying the restricting allele, and the reference annotation source (VDJdb or CMV_ECOcluster). Columns represent individual donors, grouped into HC and SuS (def) blocks. BH-adjusted *P* values (right) were derived from a linear model regressing per-individual TRB breadth on group and carrier HLA alleles for VDJdb-annotated epitopes (n = 12), or a two-sided Wilcoxon rank-sum test for CMV_ECOcluster-annotated epitopes, which were HLA-filtered upstream (n = 29). Significance levels: *P < 0.05, **P < 0.01, ***P < 0.001, ****P < 0.0001.

(B,C) Partial least-squares discriminant analysis (PLS-DA) of HC versus SuS (def) donors using CMV-epitope TRB breadth features, stratified by HLA-C*07:02 carriage: **(B)** HLA-C*07:02-positive donors (SuS, n = 19; HC, n = 26) and **(C)** HLA-C*07:02-negative donors (SuS, n = 24; HC, n = 78). Each point represents one donor projected onto the first two latent variables (LV1, LV2; the percentage of variance is shown in the axis labels); ellipses denote the 95% confidence region per group. Cross-validated classification accuracy and the number of discriminating features retained in each model are annotated, but are descriptive as the whole cohort is fitted and then plotted for illustration purposes. The annotated accuracy reflects the LOOCV loop described in Methods, not the illustrative refit shown here.

(D) Percentage of total anti-CMV TRB breadth attributable to HLA-B*07:02- or HLA-C*07:02-restricted epitopes in carriers of these alleles, HC [CMV+] versus SuS (def). *P* values were calculated by a two-sided Wilcoxon rank-sum test.

(E) Percentage of anti-CMV TRB breadth attributable to HLA class I-restricted epitopes, HC [CMV+] versus SuS (def), showing a shift toward class I-restricted ($CD8^+$ T-cell) responses in SuS (def). *P* values were calculated using a two-sided Wilcoxon rank-sum test.



968

969 **Figure 3. Convergent anti-CMV responses as well as virological and serological**
970 **assessments indicate recurrent CMV reactivation in SuS.**

971 **(A)** Force-directed network layout of one SuS patient's pooled TRB clonotypes
972 clustered by CDR3 sequence similarity. Each node represents a unique clonotype; red
973 nodes indicate CMV-annotated clonotypes; node size scales with cluster/clonal size.
974 Edges connect clonotypes within the similarity threshold (TCRdist ≤ 12) used for
975 clustering.

976 **(B)** Percentage of TRB rearrangements falling within a similarity cluster, HC [CMV+]
977 versus SuS (def). P value was calculated by a two-sided Wilcoxon rank-sum test.

(C) Percentage of TRB templates (sequenced cells) falling within CMV-associated clusters, HC [CMV+] versus SuS (def). P value was calculated using a two-sided Wilcoxon rank-sum test.

(D) Number of CMV-annotated TRB clusters per subject as a function of age, in HC (n = 102) and SuS (def, n = 43). Lines denote linear regression fits per group (shaded band, 95% confidence interval); annotated values are the Spearman correlation coefficient per group and the P value for the age × group interaction term from a linear model.

(E) Inter-donor clustering of TRB sequences. Per-cluster association plot restricted to clusters significantly enriched for patients with SuS or HC (Fisher's exact test, P < 0.05). Each point represents one TRB cluster: x-axis, percentage of CMV-annotated sequences within the cluster; y-axis, percentage of contributing patients with SuS; point size, number of individuals contributing to the cluster; color, the dominant CMV protein expression lytic phase (immediate-early, early, or late) among CMV-annotated sequences in the cluster, or unresolved where phase could not be assigned. Dashed line at 29.3%, representing the reference SuS-patient fraction within the analyzed dataset.

(F) CMV IgM titers (log10 cut-off index [COI]) among CMV IgG-positive donors, HC [CMV+] (n = 52) versus SuS (def, n = 70). Dotted line, assay positivity cut-off (COI = 0.7). P value, two-sided Wilcoxon rank-sum test. Arrow indicates the derived analyses above the clinical threshold shown in (G).

(G) Adjusted difference in probability of CMV reactivation, SuS (def, n = 70) versus HC [CMV+] (n = 52), for IgM positivity (COI >= 0.7), serum CMV DNA (PCR) positivity, and either marker positive ("any CMV activity markers"), estimated from linear mixed-effects models fitted at the visit level with a random intercept per individual to account for repeated visits, adjusted for age and sex. Points denote the adjusted difference in probability relative to HC [CMV+] (reference, dashed line at 0); error bars, 95% Wald confidence interval; P values were calculated using two-sided t-tests with Satterthwaite-approximated degrees of freedom.

(H) CMV IgM titers among donors who tested serologically IgM-negative below the clinical 0.7 cut-off, HC [CMV+] (n = 45) versus SuS (def, n = 48). Dotted line, assay positivity cut-off (COI = 0.7). P value was calculated by a two-sided Wilcoxon rank-sum test.

(I) CMV IgM titers in HC, by CMV IgG serostatus (CMV IgG-negative (n = 101) versus CMV IgG-positive (n = 50). Dotted line, assay positivity cut-off (COI = 0.7). P value was calculated by a two-sided Wilcoxon rank-sum test.

(J) Association between immunosuppressive treatment and CMV reactivation within patients with SuS (def, n = 69), modeled separately for CMV IgM positivity (left) and serum CMV DNA positivity (right). Odds ratios (points) and 95% confidence intervals

(lines) are derived from population-averaged logistic regression (generalized estimating equations, exchangeable working correlation, robust sandwich standard errors clustered on patient), with immunosuppressive exposure within the six months preceding the blood draw, age, and sex as covariates. Each model is restricted to visits at which the corresponding assay was performed.

(K) Percentage of NKG2C^{+} cells among NKG2A^{-}CD56dim NK cells (flow cytometry, gating strategy shown in Supplementary Figure 3), compared across HC [CMV IgG-negative] (n = 29), HC [CMV IgG-positive] (n = 18), and SuS (n = 41). P values were calculated by two-sided Wilcoxon rank-sum tests for the indicated pairwise comparisons.

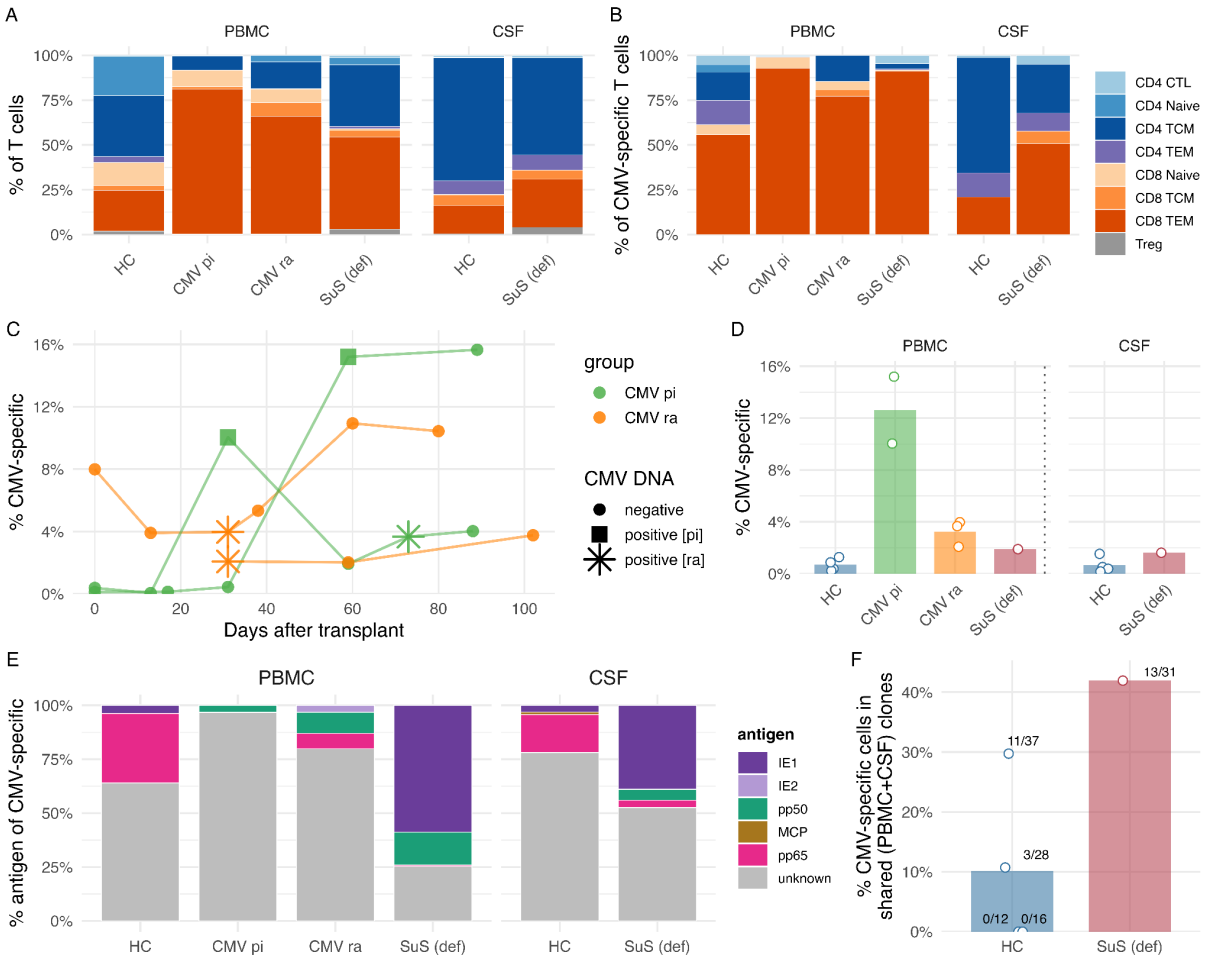


Figure 4. Single-cell profiling of a patient with SuS reveals convergent CMV-specific CD8⁺ T cell expansion paralleling CMV reactivation after allogeneic HSCT.

Combined single-cell RNA and TCRαβ sequencing of PBMC-derived and CSF-derived T cells from CMV IgG-positive (either measured or inferred) HC (n = 4) and one patient with SuS (def), integrated with an external cohort of allogeneic hematopoietic stem-cell transplant (HSCT) recipients with confirmed CMV reactivation[40] and stratified by donor CMV serostatus: CMV primary infection (pi, n = 2; CMV IgG-negative donor), and CMV reactivation (ra, n = 2; CMV IgG-positive donor). For the HSCT cohort, panel **D** shows each patient at a single cross-sectional time point at or immediately after clinically confirmed CMV reactivation (mean of both reactivation time points for the one patient sampled twice at reactivation); panel **C** shows the full longitudinal course. CMV-specific T cells were identified by matching TRB sequences to reference CMV-epitope databases at strict stringency.

(A) T-cell subset composition ($CD4^+$ CTL, naive, TCM, TEM; $CD8^+$ naive, TCM, TEM; regulatory T cells [Treg]) as a percentage of all T cells, by group and tissue.

(B) CMV-specific T-cell subset composition, as a percentage of CMV-specific T cells, by group and tissue.

(C) Longitudinal course of the percentage of CMV-specific T cells (PBMC) versus days after transplant for patients with CMV pi and CMV ra. Stars mark the sample at, or nearest after, confirmed CMV DNA detection (reactivation); squares mark the sample at, or nearest after, confirmed primary CMV DNA detection.

(D) Percentage of T cells that are CMV-specific, by group and tissue. Bars denote the group mean (HC, CMV pi, and CMV ra are means across individuals; SuS (def) is a single donor profiled at single-cell resolution); points denote individual donors.

(E) CMV-specific T-cell antigen specificity (IE1, IE2, pp50, MCP, pp65, assigned from TRB-epitope reference annotation; unknown, CMV-associated but protein unresolved), as a percentage of CMV-specific T cells, by group and tissue.

(F) Percentages and numbers of CMV-specific T-cell clones detected in both PBMC and CSF ("shared"), as a percentage of all CMV-specific clones, in HC and SuS (def) only.

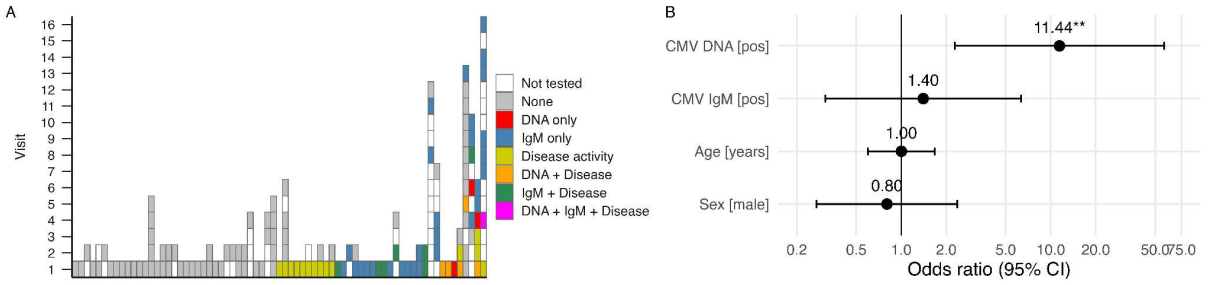


Figure 5. Visit-level co-occurrence of CMV reactivation and disease activity in definite SuS.

(A) Longitudinal tile plot of virologic and disease activity status at each study visit for every patient with definite SuS (one column per patient, n = 63, ordered by CMV DNAemia, then IgM positivity, then overall marker burden; one row per visit). Each tile is colored by the combined status at that visit: no positive marker and no evidence of disease activity (None); CMV DNAemia alone (DNA only); CMV IgM alone (IgM only); disease activity alone (Disease activity); or their pairwise and triple combinations (DNA + Disease, IgM + Disease, DNA + IgM + Disease). Marker positivity is defined only where the corresponding assay was performed: visits at which neither serum CMV DNA nor CMV IgM was measured are shown in white ("Not tested").

(B) Forest plot of odds ratios (points) and 95% confidence intervals (lines; robust sandwich estimator, cluster-adjusted for repeated visits per patient) from a population-averaged logistic regression (generalized estimating equations, exchangeable working correlation) modeling visit-level disease activity as a function of CMV DNAemia (CMV DNA [pos]), CMV IgM positivity (IgM [pos]), age, and sex. The analysis is restricted to visits at which both assays were performed and disease activity was documented (n = 111 visits from 63 patients). ** = $P < 0.01$.

References

1. Susac, J. O., Hardman, J. M. & Selhorst, J. B. Microangiopathy of the brain and retina. *Neurology* **29**, 313–313 (1979).

2. Kleffner, I. *et al.* Diagnostic criteria for Susac syndrome. *J Neurol Neurosurg Psychiatry* **87**, 1287–1295 (2016).

3. Gross, C. C. *et al.* CD8+ T cell-mediated endotheliopathy is a targetable mechanism of neuro-inflammation in Susac syndrome. *Nat Commun* **10**, 5779 (2019).

4. Bjornevik, K. *et al.* Longitudinal analysis reveals high prevalence of Epstein-Barr virus associated with multiple sclerosis. *Science* **375**, 296–301 (2022).

5. Lanz, T. V. *et al.* Clonally expanded B cells in multiple sclerosis bind EBV EBNA1 and GlialCAM. *Nature* **603**, 321–327 (2022).

6. ElAbd, H. *et al.* T and B cell responses against Epstein–Barr virus in primary sclerosing cholangitis. *Nat Med* 1–11 (2025) doi:10.1038/s41591-025-03692-w.

7. Younis, S. *et al.* Epstein-Barr virus reprograms autoreactive B cells as antigen-presenting cells in systemic lupus erythematosus. *Sci. Transl. Med.* **17**, eady0210 (2025).

8. Dörr, J. *et al.* Characteristics of Susac syndrome: a review of all reported cases. *Nat Rev Neurol* **9**, 307–316 (2013).

9. Laird, P. W., Newman, N. J. & Yeh, S. Exacerbation of Susac Syndrome Retinopathy by Interferon Beta-1a. *Arch Ophthalmol* **130**, 804–806 (2012).

10. Schneider-Hohendorf, T. *et al.* Broader Epstein–Barr virus–specific T cell receptor repertoire in patients with multiple sclerosis. *Journal of Experimental Medicine* **219**, e20220650 (2022).

11. Bjornevik, K. *et al.* CD4+ T cells reactive to Epstein-Barr virus late lytic antigens are enriched in individuals with multiple sclerosis. *Science Translational Medicine* **18**, eadz6566 (2026).

12. Schwarz, T. *et al.* An Interferon-Gamma Release Assay for Monitoring of T-Cell responses to Epstein-Barr Virus: Application to Multiple Sclerosis. *Journal of Clinical Virology* 105987 (2026) doi:10.1016/j.jcv.2026.105987.

13. Schneider-Hohendorf, T. *et al.* Broader anti-EBV TCR repertoire in multiple sclerosis: disease specificity and treatment modulation. *Brain* awae244 (2024) doi:10.1093/brain/awae244.

14. Petty, G. W. *et al.* Retinocochleocerebral vasculopathy. *Medicine (Baltimore)* **77**, 12–40 (1998).

15. Wilf-Yarkoni, A. *et al.* Increased incidence of Susac syndrome: a case series study. *BMC Neurol* **20**, 332 (2020).

16. Zuhair, M. *et al.* Estimation of the worldwide seroprevalence of cytomegalovirus: A systematic review and meta-analysis. *Reviews in Medical Virology* **29**, e2034 (2019).

17. Söderberg-Nauclér, C., Fish, K. N. & Nelson, J. A. Reactivation of Latent Human Cytomegalovirus by Allogeneic Stimulation of Blood Cells from Healthy Donors. *Cell* **91**, 119–126 (1997).

18. Sylwester, A. W. *et al.* Broadly targeted human cytomegalovirus-specific CD4+ and CD8+ T cells dominate the memory compartments of exposed subjects. *J Exp Med* **202**, 673–685 (2005).

19. Grefte, A., Giessen, M. van der, Son, W. van & The, T. H. Circulating Cytomegalovirus (CMV)-Infected Endothelial Cells in Patients with an Active CMV Infection. *J Infect Dis* **167**, 270–277 (1993).

20. Munks, M. W. *et al.* Latent CMV infection of Lymphatic endothelial cells is sufficient to drive CD8 T cell memory inflation. *PLoS Pathog* **19**, e1010351 (2023).

21. Arnaout, R. A., Prak, E. T. L., Schwab, N., Rubelt, F. & Adaptive Immune Receptor Repertoire, C. The Future of Blood Testing Is the Immunome. *Front Immunol* **12**, 626793 (2021).

22. Meyer zu Hörste, G., Gross, C. C., Klotz, L., Schwab, N. & Wiendl, H. Next-Generation Neuroimmunology: New Technologies to Understand Central Nervous System Autoimmunity. *Trends in Immunology* **41**, 341–354 (2020).

23. Jarius, S. *et al.* Update on the diagnosis and treatment of neuromyelits optica spectrum disorders (NMOSD) – revised recommendations of the Neuromyelitis Optica Study Group (NEMOS). Part I: Diagnosis and differential diagnosis. *J Neurol* **270**, 3341–3368 (2023).

24. Banwell, B. *et al.* Diagnosis of myelin oligodendrocyte glycoprotein antibody-associated disease: International MOGAD Panel proposed criteria. *The Lancet Neurology* **22**, 268–282 (2023).

25. Musvosvi, M. *et al.* T cell receptor repertoires associated with control and disease progression following Mycobacterium tuberculosis infection. *Nat Med* **29**, 258–269 (2023).

26. Nolan, S. *et al.* A large-scale database of T-cell receptor beta sequences and binding associations from natural and synthetic exposure to SARS-CoV-2. *Front. Immunol.* **16**, (2025).

27. May, D. H. *et al.* Immune signatures of common exposures through co-occurrence of T-cell receptors in tens of thousands of donors. 2024.03.26.583354 Preprint at https://doi.org/10.1101/2024.03.26.583354 (2026).

28. Lachmann, R. *et al.* Cytomegalovirus (CMV) seroprevalence in the adult population of Germany. *PLoS ONE* **13**, e0200267 (2018).

29. Emerson, R. O. *et al.* Immunosequencing identifies signatures of cytomegalovirus exposure history and HLA-mediated effects on the T cell repertoire. *Nat Genet* **49**, 659–665 (2017).

30. May, D. H., Woodhouse, S., Howie, B. & Robins, H. S. A Catalog of the Public T-cell Response to Cytomegalovirus. 2024.05.08.593237 Preprint at https://doi.org/10.1101/2024.05.08.593237 (2024).

31. Rawat, P. *et al.* Identification of a type 1 diabetes–associated T cell receptor repertoire signature from the human peripheral blood. *Science Advances* **12**, eadx7448 (2026).

32. Goncharov, M. *et al.* VDJdb in the pandemic era: a compendium of T cell receptors specific for SARS-CoV-2. *Nat Methods* **19**, 1017–1019 (2022).

33. Zahid, H. J., May, D., Robins, H. & Greissl, J. A fundamental relationship between TCR diversity, repertoire size and systemic clonal expansion: insights from 30,000 TCRβ repertoires. *Front. Immunol.* **16**, 1707727 (2026).

34. Minervina, A. A. *et al.* SARS-CoV-2 antigen exposure history shapes phenotypes and specificity of memory CD8+ T cells. *Nat Immunol* **23**, 781–790 (2022).

35. *Klinische Liquordiagnostik: Mit Zytologieatlas*. (De Gruyter, 2024). doi:10.1515/9783110331905.

36. Griffiths, P. & Reeves, M. Pathogenesis of human cytomegalovirus in the immunocompromised host. *Nat Rev Microbiol* **19**, 759–773 (2021).

37. Gumá, M. *et al.* Imprint of human cytomegalovirus infection on the NK cell receptor repertoire. *Blood* **104**, 3664–3671 (2004).

38. Falk, S. *et al.* Single-cell analysis of skin and blood reveals systemic immune responses to ultraviolet B and their impairment in MS. *J Neuroinflammation* **23**, 210 (2026).

39. Pappalardo, J. L. *et al.* Transcriptomic and clonal characterization of T cells in the human central nervous system. *Sci Immunol* **5**, eabb8786 (2020).

40. Häkkinen, A.-E. *et al.* Single-Cell Analysis of Adaptive NK and CMV-Specific T Cell Dynamics after Allogeneic HSCT. *Blood Advances* https://doi.org/10.1182/bloodadvances.2026019733 (2026) doi:10.1182/bloodadvances.2026019733.

41. Roback, J. D. *et al.* CMV DNA is rarely detected in healthy blood donors using validated PCR assays. *Transfusion* **43**, 314–321 (2003).

42. Drew, W. L. Cytomegalovirus Resistance Testing: Pitfalls and Problems for the Clinician. *Clin Infect Dis* **50**, 733–736 (2010).

43. Fowler, K. B. *et al.* The Outcome of Congenital Cytomegalovirus Infection in Relation to Maternal Antibody Status. *New England Journal of Medicine* **326**, 663–667 (1992).

44. Goderis, J. *et al.* Hearing Loss and Congenital CMV Infection: A Systematic Review. *Pediatrics* **134**, 972–982 (2014).

45. Pachnio, A. *et al.* Cytomegalovirus Infection Leads to Development of High Frequencies of Cytotoxic Virus-Specific CD4+ T Cells Targeted to Vascular Endothelium. *PLOS Pathogens* **12**, e1005832 (2016).

46. Daida, K. *et al.* Cytomegalovirus-associated encephalomyelitis in an immunocompetent adult: a two-stage attack of direct viral and delayed immune-mediated invasions. case report. *BMC Neurol* **16**, 223 (2016).

47. Reddy, V., Lodha, L., Gupta, S., Mani, R. S. & Ashwini, M. A. Neurological Consequences of CMV Infection: Overview of Pathogenesis and Host Responses. *Reviews in Medical Virology* **36**, e70095 (2026).

48. Roullet, E. Opportunistic infections of the central nervous system during HIV-1 infection (emphasis on cytomegalovirus disease). *J Neurol* **246**, 237–243 (1999).

49. Abrahamyan, S. *et al.* Complete Epstein-Barr virus seropositivity in a large cohort of patients with early multiple sclerosis. *J Neurol Neurosurg Psychiatry* **91**, 681–686 (2020).

50. Levin, L. I., Munger, K. L., O'Reilly, E. J., Falk, K. I. & Ascherio, A. Primary infection with the Epstein-Barr virus and risk of multiple sclerosis. *Annals of Neurology* **67**, 824–830 (2010).

51. Schlott, F. *et al.* Characterization and clinical enrichment of HLA-C*07:02-restricted Cytomegalovirus-specific CD8+ T cells. *PLOS ONE* **13**, e0193554 (2018).

52. Ameres, S. *et al.* Presentation of an Immunodominant Immediate-Early CD8+ T Cell Epitope Resists Human Cytomegalovirus Immunoevasion. *PLOS Pathogens* **9**, e1003383 (2013).

53. Aydin, S., Pareja, J., Liblau, R. & Engelhardt, B. Antigen presentation at the blood-brain barrier amplifies neuroinflammation. *Trends Immunol* S1471-4906(26)00185–7 (2026) doi:10.1016/j.it.2026.07.006.

54. Thomas, O. G. *et al.* Anoctamin-2-specific T cells link Epstein-Barr virus to multiple sclerosis. *Cell* **0**, (2026).

55. Thomas, O. G. *et al.* Cross-reactive EBNA1 immunity targets alpha-crystallin B and is associated with multiple sclerosis. *Science Advances* **9**, eadg3032 (2023).

56. Vietzen, H. *et al.* Accumulation of Epstein-Barr virus–induced cross-reactive immune responses is associated with multiple sclerosis. *J Clin Invest* **134**, (2024).

57. Willekens, B. & Kleffner, I. Susac syndrome and pregnancy: a review of published cases and considerations for patient management. *Ther Adv Neurol Disord* **14**, 1756286420981352 (2021).

58. Cannon, M. J., Hyde, T. B. & Schmid, D. S. Review of cytomegalovirus shedding in bodily fluids and relevance to congenital cytomegalovirus infection. *Reviews in Medical Virology* **21**, 240–255 (2011).

59. Maguire, C. *et al.* Virus reactivation in acute and long COVID-19. *Nature* **656**, 700–711 (2026).

60. Bianco, A. *et al.* New onset of Susac syndrome after mRNA COVID-19 vaccine: a case report. *Journal of Neurology* **270**, 614–617 (2023).

61. Chen, P.-J., Chang, Y.-S., Lim, C.-C. & Lee, Y.-K. Susac Syndrome Following COVID-19 Vaccination: A Case Report. *Vaccines* **10**, 363 (2022).

62. Fisher, L., David, P., Sobeh, T., Liberman, R. B. & Amital, H. Susac syndrome following COVID-19 vaccination: a case-based review. *Clinical Rheumatology* **42**, 1713–1717 (2023).

63. Raymaekers, V. *et al.* Susac syndrome complicating a SARS-CoV-2 infection. *Journal of NeuroVirology* **27**, 954–959 (2021).

64. Tsitos, S., Danek, A. & Straube, A. Susac syndrome in a patient with migraine shortly after COVID-19 booster vaccination: more than a temporal relation? *Journal of Neurology* **271**, 71–74 (2024).

65. Venditti, L., Rousseau, A., Ancelet, C., Papo, T. & Denier, C. Susac syndrome following COVID-19 infection. *Acta Neurologica Belgica* **121**, 807–809 (2021).

66. Waldman, W. J. *et al.* NOVEL MECHANISM OF INHIBITION OF CYTOMEGALOVIRUS BY THE EXPERIMENTAL IMMUNOSUPPRESSIVE AGENT LEFLUNOMIDE1,2: *Transplantation* **68**, 814–825 (1999).

67. Zheng, K. *et al.* Leflunomide: Traditional immunosuppressant with concurrent antiviral effects. *Int J Rheum Dis* **26**, 195–209 (2023).

68. Mateen, F. J. *et al.* Susac syndrome: clinical characteristics and treatment in 29 new cases. *European Journal of Neurology* **19**, 800–811 (2012).

69. Moheb, N. *et al.* Outcomes of Maintenance Immunotherapy in a Cohort of Patients With Susac Syndrome. *Neurology Clinical Practice* **15**, e200544 (2025).

70. Goldstein, G. *et al.* The role of immunoglobulin prophylaxis for prevention of cytomegalovirus infection in pediatric hematopoietic stem cell transplantation recipients. *Pediatr Blood Cancer* **64**, (2017).

71. Alexander, B. T. *et al.* Use of Cytomegalovirus Intravenous Immune Globulin for the Adjunctive Treatment of Cytomegalovirus in Hematopoietic Stem Cell Transplant Patients. *Pharmacotherapy* **30**, 554–561 (2010).

72. Eichholz, J. C., Bremer, B., Wedemeyer, H., Maasoumy, B. & Sandmann, L. Clinical evaluation of the Altostar HDV RT-PCR Kit 1.5. *Journal of Clinical Virology* **185**, 105971 (2026).

73. Łacina, P. *et al.* miR-302d-3p expression and genotype are associated with CMV replication after allogeneic haematopoietic stem cell transplantation. *Human Immunology* **86**, 111599 (2025).

74. Dash, P. *et al.* Quantifiable predictive features define epitope-specific T cell receptor repertoires. *Nature* **547**, 89–93 (2017).

75. Klinger, M. *et al.* Multiplex Identification of Antigen-Specific T Cell Receptors Using a Combination of Immune Assays and Immune Receptor Sequencing. *PLOS ONE* **10**, e0141561 (2015).

76. Hahsler, M., Piekenbrock, M. & Doran, D. dbscan: Fast Density-Based Clustering with R. *Journal of Statistical Software* **91**, 1–30 (2019).

77. Orenbuch, R. *et al.* arcasHLA: high-resolution HLA typing from RNAseq. *Bioinformatics* **36**, 33–40 (2020).

78. Grabauskas, T. *et al.* CMV-specific clonal expansion in human Th1 and GZMK^{+} CD8^{+} T cells. *Genome Biol* https://doi.org/10.1186/s13059-026-04198-5 (2026) doi:10.1186/s13059-026-04198-5.

79. Korsunsky, I. *et al.* Fast, sensitive and accurate integration of single-cell data with Harmony. *Nat Methods* **16**, 1289–1296 (2019).

80. Benjamini, Y. & Hochberg, Y. Controlling the False Discovery Rate: A Practical and Powerful Approach to Multiple Testing. *Journal of the Royal Statistical Society: Series B (Methodological)* **57**, 289–300 (1995).

Supplement

Supplementary table 1

	SuS	HC	Significance
CMV IgG/IgM serology			
n	70	162	
CMV IgG-positive	70 (100%; 95% CI 94.9-100%)	54 (33%; 95% CI 26.24-40.43%)	*P* < 2.22e-16
Age	36.4 (95% CI 34.0-38.8)	35.4 (95% CI 33.5-37.4)	*P* = 0.10
Sex (f:m)	49:21 (2.33)	116:46 (2.52)	*P* = 0.87
CMV serum DNAemia			
n	70	54	
CMV IgG-positive	70 (100%)	54 (100%)	
Age	36.2 (95% CI 33.8-38.6)	38.5 (95% CI 35.1-41.8)	*P* = 0.43
Sex (f:m)	49:21 (2.33)	41:13 (3.15)	*P* = 0.54
TRB sequencing			
n	43	104	
CMV IgG-positive	43 (100%)	104 (100%)	
Age	36.6 (95% CI 33.6-39.5)	37.2 (95% CI 35.0-39.3)	*P* = 0.82
Sex (f:m)	29:14 (2.07)	68:36 (1.89)	*P* = 0.85

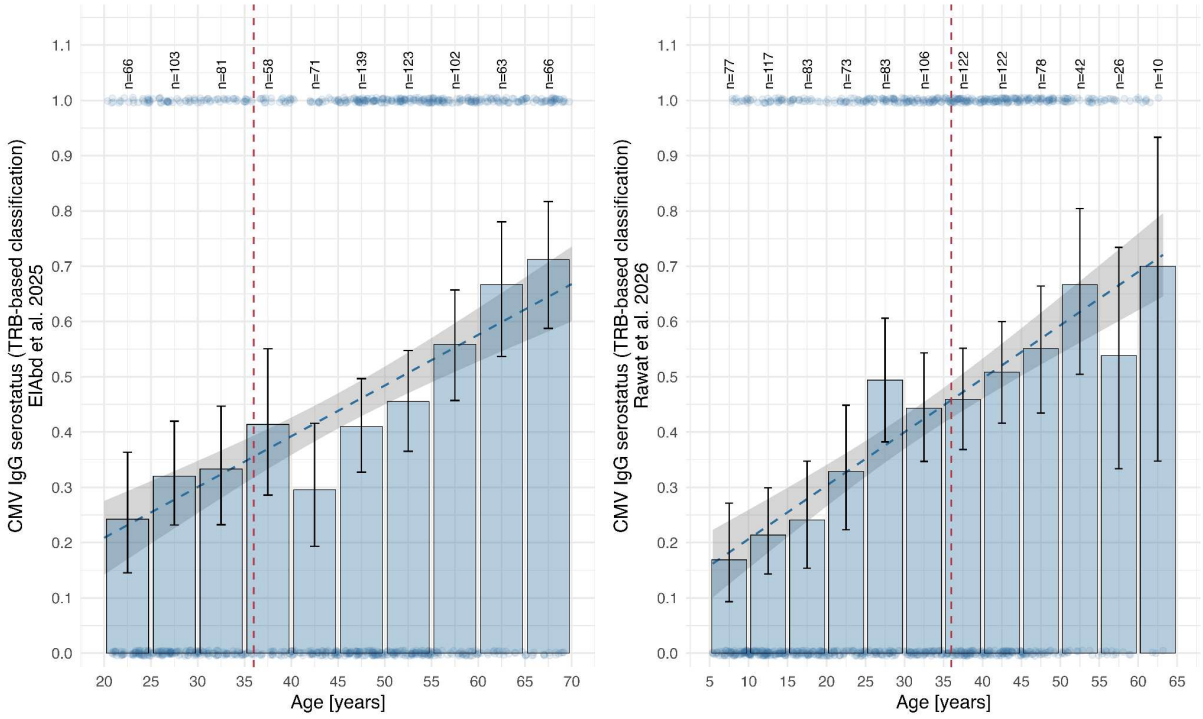
Supplementary table 2

Feature	Number of TRB MIRA sequences	Peptide	Protein	Phase
feature11611_B_35_01	69	IPSINVHHY	pp65	Late

feature11611_B_35_01	26	SEHPTFTSQY	pp65	Late
feature14970_B_40_01	25	YAYIHTTYL	gB	Late
feature17945_B_51_01	7	LPYPRGYTL	UL26	Unknown
feature20022_C_04_01	11	FVFDNARLV	UL112	Unknown
feature20410_B_07_02	6	TPRVTGGGAM	pp65	Late
feature20414_C_07_02	32	CRVLCCYVL	IE-1	Immediate-Early
feature20419_C_07_02	10	CRVLCCYVL	IE-1	Immediate-Early
feature20421_C_07_02	8	CRVLCCYVL	IE-1	Immediate-Early
feature29890_DQA1_01_01+DQB1_05_01	9	LPLKMLNIPSINVH	pp65	Late
feature3296_A_24_02	26	SYAQKIFKI	IE-1	Immediate-Early
feature339_A_01_01	82	YADPFFLKY	UL105	Early
feature339_A_01_01	26	VTEHDTLLY	ORFL112C	Unknown
feature339_A_01_01	8	SEHPTFTSQY	pp65	Late
feature339_A_01_01	7	RTDPATLTAY	UL69	Early
feature342_A_01_01	13	RTDPATLTAY	UL69	Early
feature342_A_01_01	11	YADPFFLKY	UL105	Early
feature342_A_01_01	8	SEHPTFTSQY	pp65	Late
feature342_A_01_01	7	VTEHDTLLY	ORFL112C	Unknown
feature343_A_01_01	17	YADPFFLKY	UL105	Early
feature37525_DRB1_07_01	44	PDDYSNTHSTRYVTV	gB	Late
feature37525_DRB1_07_01	10	LPLKMLNIPSINVH	pp65	Late
feature37525_DRB1_07_01	9	EPDVYYTSAFVFPTK	pp65	Late
feature40348_DRB1_12_01	17	LPLKMLNIPSINVH	pp65	Late
feature689_A_02_01	43	NLVPMVATV	pp65	Late
feature689_A_02_01	28	GVLDAVWRV	US8	Unknown
feature689_A_02_01	12	ALWDVALLEV	ORFL321W	Unknown
feature689_A_02_01	8	FMDILTTCVET	IE-1	Immediate-Early
feature689_A_02_01	6	YLDSMAIFL	US20	Unknown
feature689_A_02_01	6	CLLESVYTA	TP	Late
feature7900_B_07_02	6	TPRVTGGGAM	pp65	Late
feature8029_B_08_01	24	QIKVRVDMV	IE-1	Immediate-Early
feature9526_B_15_01	11	YAYIHTTYL	gB	Late

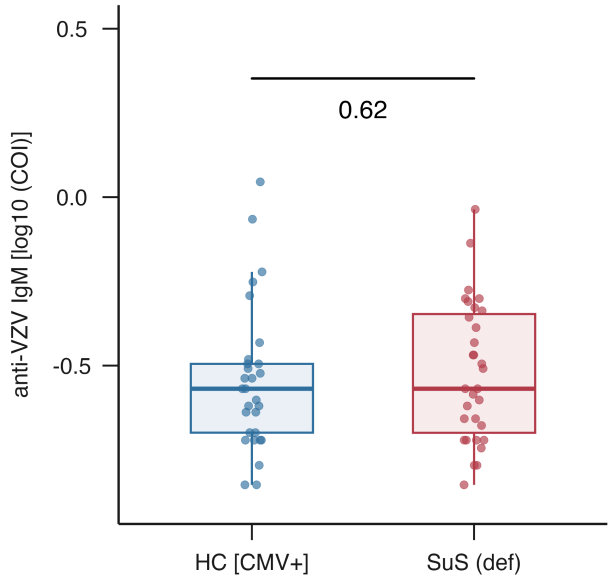
1308

Supplementary Figures:



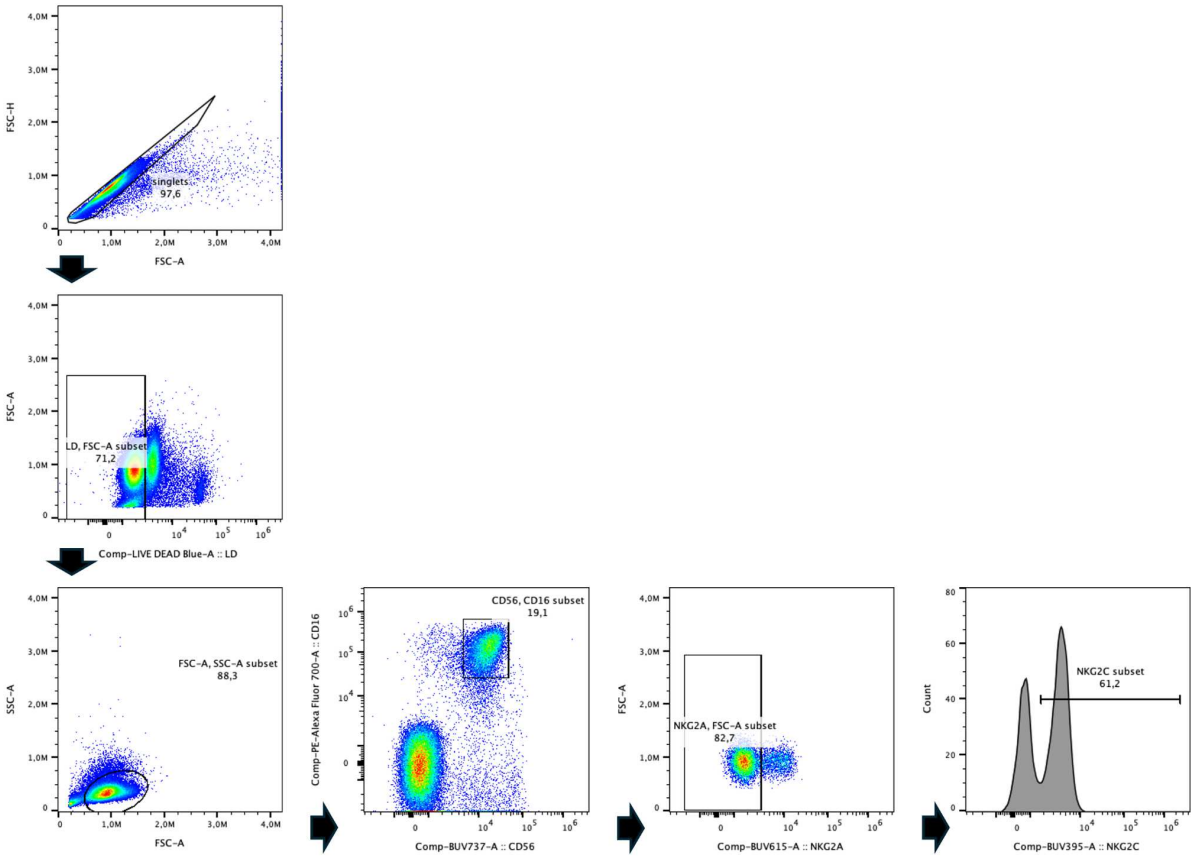
Supplementary Figure 1: CMV IgG seroprevalence by age in two independent healthy control TRB cohorts.

CMV IgG serostatus, classified from TRB repertoire data based on the frequency of CMV-annotated clonotypes relative to sequencing depth, in 872 healthy controls from (A) the ElAbd et al. cohort (Germany; ages 20–70) and (B) 939 healthy controls of the Rawat et al. cohort (USA; ages 5–65). Bars show the proportion of CMV IgG-classified-positive donors within each 5-year age bin (95% Clopper-Pearson confidence intervals); points along y = 0 and y = 1 show individual donor-level classifications (jittered for visibility). The dashed blue line and grey band show a linear regression fit with 95% confidence interval. The dashed red vertical line indicates the mean age of the SuS cohort (36 years) for reference.



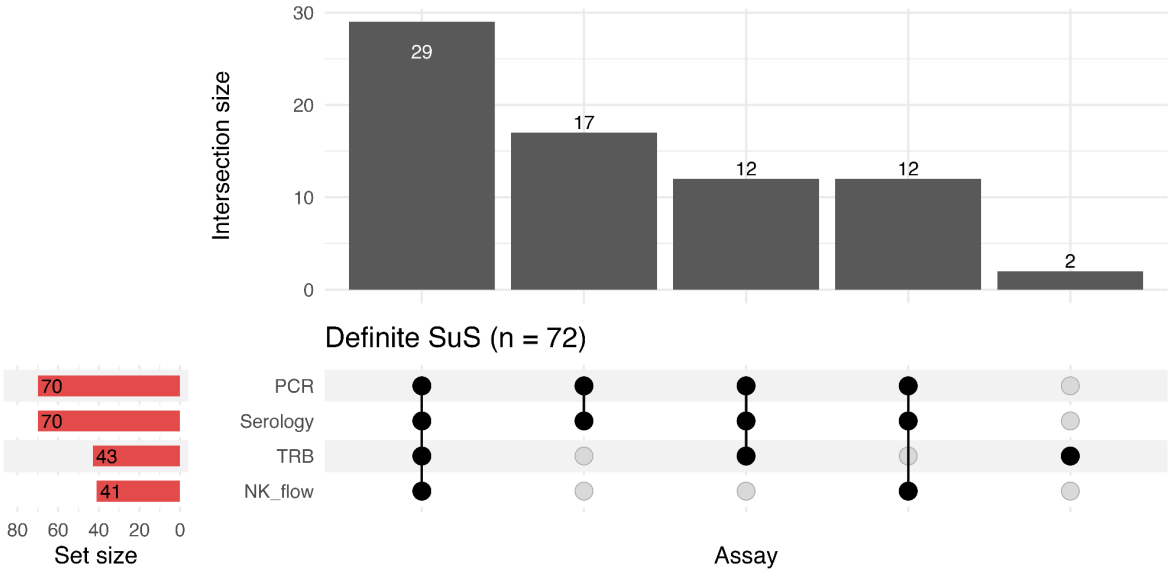
Supplementary Figure 2. Elevated IgM in Susac syndrome is not observed against varicella zoster virus (VZV).

Anti-VZV IgM titers (log10 cut-off index [COI]) in CMV IgG-positive healthy controls (HC [CMV+]) versus patients with definite Susac syndrome (SuS (def)). Boxes denote the median and interquartile range, whiskers extend to 1.5 × IQR, and individual donors are shown as points. The P value was calculated by a two-sided Wilcoxon rank-sum test.



Supplementary Figure 3: Example flow-cytometry gating

Doublet exclusion was followed by live dead gating and lymphocyte gating by size. CD56/CD16 double positive lymphocytes were gated for NKG2A-negativity before quantifying frequencies of NKG2C-positive cells.



Supplementary Figure 4. Assay coverage across the discovery cohort.

UpSet plot showing which assays were performed for each of the 72 patients with definite Susac syndrome (SuS (def)) in the discovery cohort. Horizontal bars (lower left) give the number of patients assessed by each assay (set size). Vertical bars (top) give the number of patients assessed by exactly the combination of assays indicated by the filled, connected dots below (intersection size), with counts printed above each bar; grey dots denote assays not performed in that combination. Intersections are mutually exclusive and sum to 72, and every patient contributed at least one assay.